Morphology, Morphometry and Distribution of Isolated Landforms in Southern Chryse Planitia, Mars

JGR Planets

RESEARCH ARTICLE

10.1029/2020JE006775

Morphology, Morphometry and Distribution of Isolated Landforms in Southern Chryse Planitia, Mars

Joseph D. McNeil[1], **Peter Fawdon**[1], **Matthew R. Balme**[1], **and Angela L. Coe**[2]

[1]School of Physical Sciences, The Open University, Milton Keynes, UK, [2]School of Earth, Environment and Ecosystem Sciences, The Open University, Milton Keynes, UK

Key Points:

- There is a population of >14,000 mounds in southern Chryse Planitia that we classify as hills, mesas, clustered mounds, and compound mounds
- The mounds are most likely remnants of an extensive 500 m thick Early-Mid Noachian layer, correlatable to clay-rich Mawrth Vallis strata
- Mineralization from groundwater in regions of high permeability most likely contributed to their apparent preferential preservation

Supporting Information:

Supporting Information may be found in the online version of this article.

Correspondence to:

J. D. McNeil,
joe.mcneil@open.ac.uk

Citation:

McNeil, J. D., Fawdon, P., Balme, M. R., & Coe, A. L. (2021). Morphology, morphometry and distribution of isolated landforms in southern Chryse Planitia, Mars. *Journal of Geophysical Research: Planets*, *126*, e2020JE006775. https://doi.org/10.1029/2020JE006775

Received 17 NOV 2020
Accepted 9 APR 2021

Author Contributions:

Conceptualization: Joseph D. McNeil, Peter Fawdon, Matthew R. Balme
Data curation: Joseph D. McNeil
Formal analysis: Joseph D. McNeil, Peter Fawdon
Investigation: Joseph D. McNeil
Methodology: Joseph D. McNeil, Peter Fawdon
Project Administration: Joseph D. McNeil, Peter Fawdon, Matthew R. Balme
Resources: Joseph D. McNeil

Abstract The margin of Chryse Planitia, Mars, contains >10^5 kilometer-scale mesas, buttes, and plateaus ("mounds"), many of which are found in and around Oxia Planum, the ExoMars 2022 Rover landing site. Despite this, their origins and evolution are unknown. We have analyzed the morphologies and morphometries of 14,386 individual mounds to: (1) classify them based on their geomorphology; (2) constrain when they formed based on their stratigraphic and spatial relationships; and (3) develop hypotheses for their geological history. The mounds are classified as compound mounds, mesas, clustered mounds, and hills. Mound heights show that their elevations above the plains tend to a maximum height of 500 m. We interpret this as the thickness of a previously continuous layer that extended several hundred kilometers from the southern highlands into Chryse Planitia. Stratigraphy constrains the deposition of this layer to the Early-Middle Noachian, correlatable to the phyllosilicate-bearing strata of Mawrth Vallis, with similar layering also observable in some mounds, suggesting a genetic relationship. The mounds sometimes occur in circular arrangements, interpreted as an association with buried impact structures. We propose that the mounds formed through differential erosion after the premound layer was indurated by mineralization from groundwater in areas superposing underlying crustal weaknesses, for example, at buried crater margins. The subsequent differential erosion of this layer preferentially removed areas unaffected by this induration in the Late Noachian-Early Hesperian leaving the mound population seen at present. These features present accessible three-dimensional exposures of ancient layered rocks, and so are exciting targets for future study.

Plain Language Summary Thousands of kilometer-scale "mounds" occur in the Chryse Planitia region of Mars. Until now, we did not know what they were, how old they are, or why they are so abundant. We examined the mounds, classified them based on their shape, and calculated their heights. We estimated the age of the mounds and how they formed using their relationship to other geological features nearby. We find: (1) There are four types of mounds: hills, mesas, clustered mounds, and compound mounds. (2) The mounds are never taller than about 500 m, suggesting they are remnants of a once-continuous layer about 500 m thick that has been almost completely removed. (3) Finding mounds hundreds of kilometers into Chryse Planitia means that this layer was once extensive. The largest mounds are similar to bedrock types seen around Mawrth Vallis, an area with clear mineralogical evidence of water altering the rocks in the ancient past. We think that similar minerals occur in parts of the premound layer, hardening it so that these areas were left as the mounds we see today once the rest of the layer was eroded. We conclude that the mounds are important "leftover" features from early in Mars' geological history.

1. Introduction

Oxia Planum, the landing site of the ExoMars 2022 rover "Rosalind Franklin", is a clay-rich plain located on the boundary between the ancient, rugged terrain of Arabia Terra (Quantin-Nataf et al., 2021), and the young, smooth plains of Chryse Planitia. Distributed across the Oxia Planum and wider Circum-Chryse region are thousands of kilometer-scale isolated landforms that resemble terrestrial mesas, buttes, hills, and plateaus (Figure 1). The mounds are conspicuous features that can be distinguished by their positive relief, high albedo, and low thermal inertia relative to the surrounding plains. As a widespread geomorphological feature in this highland-lowland transitional area, they are an important component of the geological history of the region, but their morphological variations, origins, and ages were hitherto not well understood. Importantly, several of these mounds are found within the landing ellipse of the ExoMars rover

Software: Joseph D. McNeil, Peter Fawdon
Supervision: Peter Fawdon, Matthew R. Balme, Angela L. Coe
Validation: Joseph D. McNeil
Visualization: Joseph D. McNeil, Peter Fawdon
Writing – original draft: Joseph D. McNeil
Writing – review & editing: Joseph D. McNeil, Peter Fawdon, Matthew R. Balme, Angela L. Coe

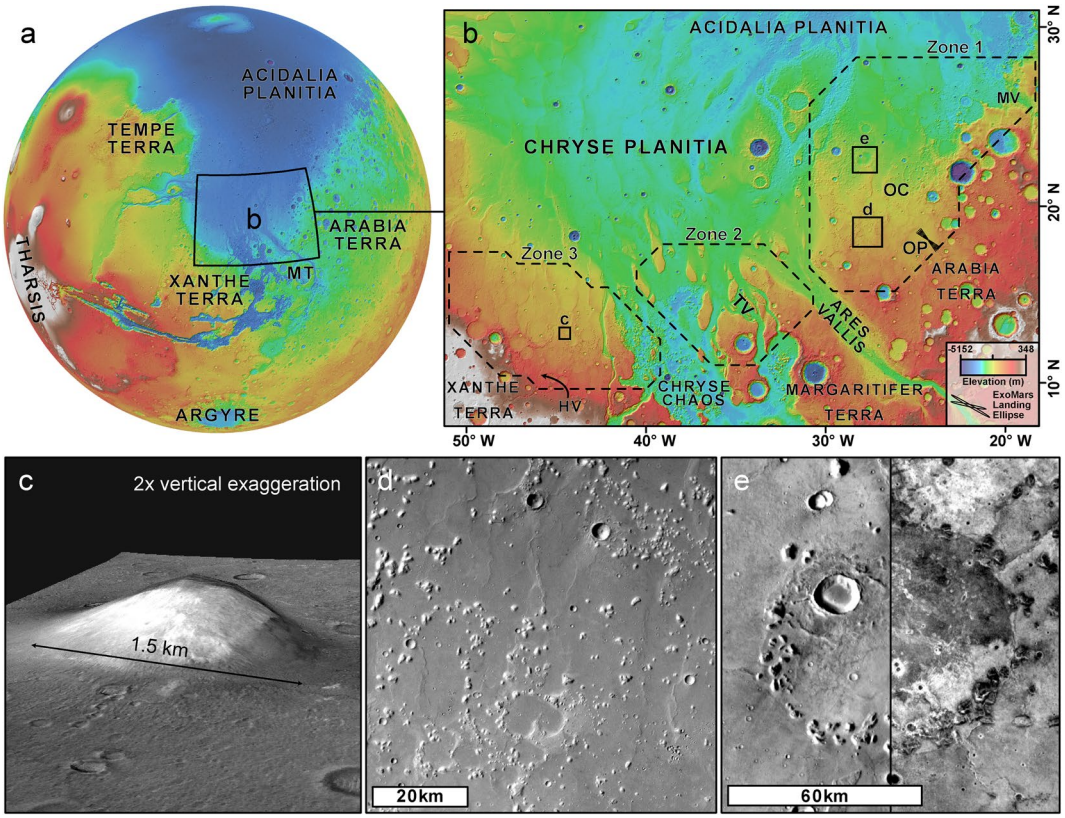

Figure 1. (a) MOLA (Mars Orbital Laser Altimeter) globe showing the position of Chryse Planitia relative to other regions of Mars. MT: Margaritifer Terra. (b) Locations of the study areas (Zones 1–3). OC: Oxia Colles, OP: Oxia Planum, TV: Tiu Valles, MV: Mawrth Vallis, HV: Hypanis Vallis. (c) 3D CTX (Context Camera) image of a 1.5 km wide isolated mound in Zone 2 showing its high albedo and rounded form. (d) Panchromatic HRSC (High Resolution Stereo Camera) image (H3081_0000_ND3) of a typical field of mounds west of Oxia Planum. (e) Left: daytime infrared THEMIS (Thermal Emission Imaging System) and right: night time THEMIS infrared image of a 70 km-diameter quasicircular arrangement of mounds (global mosaic, https://astrogeology.usgs.gov/maps/mars-themis-derived-global-thermal-inertia-mosaic), showing their characteristic low thermal inertia.

(Quantin-Nataf et al., 2021; Sefton-Nash et al., 2020). Here, the mounds overlie the clay bearing terrains that are central to the rover's primary objectives of biosignature detection and the investigation of ancient aqueous environments (Vago et al., 2017). Thus, an understanding of the formation and evolution of the mounds has direct consequences for the geology of the landing site.

Earth's sedimentary rock record forms an archive of past physical, chemical, and biological processes and conditions. This archive is subject to continual modification and destruction through surface processes and plate movements. Mars, in the absence of plate tectonics, has retained a diverse and extensive sedimentary rock record which is far older than any equivalent terrestrial sedimentary accumulation (e.g., Edgett & Malin, 2002; Grotzinger & Milliken, 2012; Malin and Edgett, 2000). On both Earth and Mars, in eroding environments where competent lithologies overlie less competent lithologies, the underlying rocks are preferentially eroded, resulting in differential down wasting and collapse of the overlying competent layer (e.g., Duszyński et al., 2019). This results in the formation of landforms such as mesas, buttes, and plateaus (Migoń, 2004). Nascent mesas and plateaus on Earth typically have steep scarps which form as the terrain begins to transition from flat to rugged, but continued erosion gradually causes their margins to become more rounded over time. Continued back wasting of these unstable scarps diminishes the areal exposure of more resistant rocks, leaving smaller, more isolated patches of resistant lithologies upstanding in the terrain. These isolated landforms record the depositional environment as well as the erosional history of the region.

In this study, for the first time, we systematically (i) identify and classify 14,386 mounds on the margin of Chryse Planitia, (ii) characterize the morphometry of the mounds by measuring their areal extents and calculating their heights, and (iii) observe the stratigraphic context of the mounds to constrain their depositional and erosional history. From these initial findings, we discuss their possible formation, diagenetic, and erosional histories, and consider the implications of these on the geological history of the Chryse-Arabia margin and specifically their significance for Oxia Planum and the ExoMars rover mission.

2. Geography and Geology of the Study Area

The mounds are geographically constrained to the areas around the southern margin of Chryse Planitia and the northern margin of Arabia Terra. Chryse Planitia is bounded on its southern rim by heavily cratered highland material; Arabia Terra lies to its southeast and Xanthe Terra lies to its southwest (Figure 1; e.g., Frey & Schultz, 1988; Greeley et al., 1977). In the north, it shares a gradational boundary with the plains of Acidalia Planitia. The materials that fill Acidalia Planitia (e.g., Pan et al., 2017) could obscure further mounds. Chryse Planitia is thought to have formed as the result of a large impact event (Frey, 2006; Schultz et al., 1982), and is generally accepted as a type example of an ancient (>4.0 Ga), infilled, and highly degraded impact basin (Pan et al., 2019). The exceptional size of Chryse Planitia, as well as its close proximity to the southern highlands, means it probably acted as a sedimentary sink for much of the detritus shed from the surrounding highland material (Oehler & Allen, 2010). Multiple prominent northward-flowing outflow channels such as Ares Valles debouch into Chryse Planitia and dissect the ancient highlands that encompass its southern margin.

To the south-west of Chryse Planitia, the wider Oxia region, including Oxia Planum and Oxia Colles, is delineated in the west by Ares Vallis, and in the east by Mawrth Vallis (Figure 1), a 600 km-long Noachian-age valley that incises phyllosilicate-rich material on the margin of the southern highlands (e.g., Loizeau et al., 2007, 2011). In comparison with other Noachian terrains, the topographies of Oxia Colles and Oxia Planum are relatively smooth and flat. The extensive plains-forming clay-rich material that characterizes Oxia Planum was probably emplaced around 4 Gy (Fawdon et al., 2020; Quantin-Nataf et al., 2021). Examples of mounds occur in Oxia Planum, however, they become more common to the north, north-east, and west, particularly in Oxia Colles, where there are thousands of well-preserved examples.

The study area encompasses the southern highland margin of Chryse Planitia and extends to the east along the dichotomy boundary to include Mawrth Vallis in the northeast. The outflow channels of Ares Valles, Chryse Chaos, and Tiu Valles dissect the study area into three conveniently sized subareas (Zone 1–3; Figure 1). Zone 1, with surface area >332,000 km^2, encompasses Oxia Planum, Oxia Colles, and the area west of Mawrth Valles. Zone 2 (>78,000 km^2) has the fewest mounds, and includes the areas of elongated islands within Chryse Chaos, Ares Vallis, and Tiu Valles, as well as the north-western extreme of the Margaritifer Terra plateau. Zone 3 (>150,000 km^2) lies west of Chryse Chaos, and includes the north-eastern section of Xanthe Terra, encompassing the mound-dense region north of Hypanis Valles. The western extent of the study area was taken to be the boundary beyond which no more mounds occurred. The northern extent of Zone 1 is a line of latitude at 28.170°N in Zone 1, where the mounds become too numerous to count and where superposing glacial deposits cause the mound morphology to become indistinct.

3. Previous Work

The mounds of southern Chryse Planitia have previously been referred to as buttes, mesas, and knobs, irrespective of their morphologies (e.g., Fawdon et al., 2018; Loizeau et al., 2012; Michalski & Noe Dobrea, 2007; Quantin-Nataf et al., 2021; Rodríguez et al., 2007). In the wider literature, these terms denote specific geographic features, so here we use the simple umbrella term "mound" to describe all the isolated, positive relief landforms in the study area. Characteristics of the mounds have been described before (Quantin-Nataf et al., 2021); however, no quantitative study of their distributions or morphologies exists. The mounds near the ExoMars landing site in Oxia Planum appear to be layered and are interpreted as remnants of younger overlying sedimentary deposits that either formed as isolated features or a more widespread regional deposit (Quantin-Nataf et al., 2021). Curvilinear features observed on their surfaces are interpreted as infilled fractures.

S. Rotto and Tanaka (1995) used Viking images to interpret the broad mound-containing region to consist of two intergrading units of "knobby terrain," dating from the Middle to Late Hesperian. They suggest two phases of knobby terrain formation: the first in the Late Noachian concurrent with Mawrth Vallis incision, and a second in the Early to Middle Hesperian. In Oxia Planum, the mounds overlie the ~4.0 Ga clay-bearing materials that are a primary target for the ExoMars 2020 rover (Quantin-Nataf et al., 2021). Some of the mounds in Zone 3 also appear to overlie sections of the Hypanis Vallis terminal fan delta, a > 970 km^2 Late Noachian-Early Hesperian sediment fan (Adler et al., 2019; Fawdon et al., 2018; Hauber et al., 2009). Some sections of the delta may be considerably older than this age, however, so this cannot be reliably used to constrain the age of the mounds (Fawdon et al., 2018).

The "knobby terrain" units that are mapped and described in S. Rotto and Tanaka (1995) are postulated to be comprised of "debris flow" material that originated from the south. They suggest the mounds themselves consist of highly degraded crater rims or other isolated peaks comprising highland plateau material, with the embaying interknob dark plains material interpreted as "reworked deposits" and lava flows (S. L. Rotto & Tanaka, 1991; S. Rotto &Tanaka, 1995). Rodríguez et al. (2007) suggest that the mounds on the boundary between Xanthe Terra and Chryse Planitia (i.e., in our Zone 3) could have been formed by a variety of processes including thermokarst activity, sedimentary volcanism, or groundwater sapping and runoff. They suggest that near-surface groundwater emergence along densely packed faults could have played a role in mound creation.

Michalski and Noe Dobrea (2007) note that a population of mounds in the area near the mouth of Mawrth Vallis exhibit clay-bearing layers in their exposed flanks that resemble those found in the Mawrth Vallis plateau (e.g., Loizeau et al., 2012, 2007; Noe Dobrea et al., 2009; Poulet et al., 2020, 2008). This suggests that these mounds are the erosional remnants of the Mawrth Vallis plateau, and probably formed early in Mars' history (Early-Middle Noachian; Loizeau et al., 2012). These clay-bearing mounds are surrounded by dark, smooth material that lacks the aqueous alteration observed in the Mawrth Vallis plateau strata (Loizeau et al., 2007). This dark plains-forming material pervades the Chryse Planitia region and corresponds to the Late Noachian-Early Hesperian $HNCc_1$ and Late Hesperian HCc_2 units of Tanaka et al., (2005). The source of this dark material is uncertain, but the lack of aqueous alteration signatures and presence of pyroxene in spectral data (Loizeau et al., 2007) suggest that these plains may be of volcanic or volcaniclastic origin. Loizeau et al. (2012) measured the crater retention model age of these dark plains, finding that they were emplaced ~3.55 Gy, which is in agreement with estimated ages of the $HNCc_1$ unit (Tanaka et al., 2005). Despite the observation that the dark plains material embays the mounds in the mouth of Mawrth Vallis (Loizeau et al., 2012), the relationship between the mounds and the plains material elsewhere along the flanks of Chryse Planitia is still unclear.

4. Data and Methods

The morphologies, morphometries, and distributions of the 14,386 mounds within Zones 1–3 (combined area of ~550,000 km^2; Figure 1b) were systematically investigated using appropriate remote sensing data. The mounds were identified by their dark toned appearance in nighttime infrared THEMIS (Thermal Emission Imaging System; Christensen et al., 2002; Fergason et al., 2006) data, suggesting that they are composed of material with relatively low thermal inertia. The mounds are bright in panchromatic CTX (Context Camera; Malin et al., 2007) images and pale toned in color HRSC (High Resolution Stereo Camera; Jaumann et al., 2007) data. The elevation of the mounds above the plains of Chryse Planitia is only observable in Mars orbital laser altimeter (MOLA) data, where point ground tracks intersect the mounds. However, HRSC digital elevation model (DEMs) are of sufficient resolution and vertical precision to resolve the shape of the mounds. Where available, HiRISE (High Resolution Imaging Science Experiment; McEwen et al., 2007) data were also used to gain a more detailed understanding of stratigraphic relationships and surface textures. All these data were incorporated into a GIS (Geographical Information Systems) project using ArcGIS 10.5.1 software.

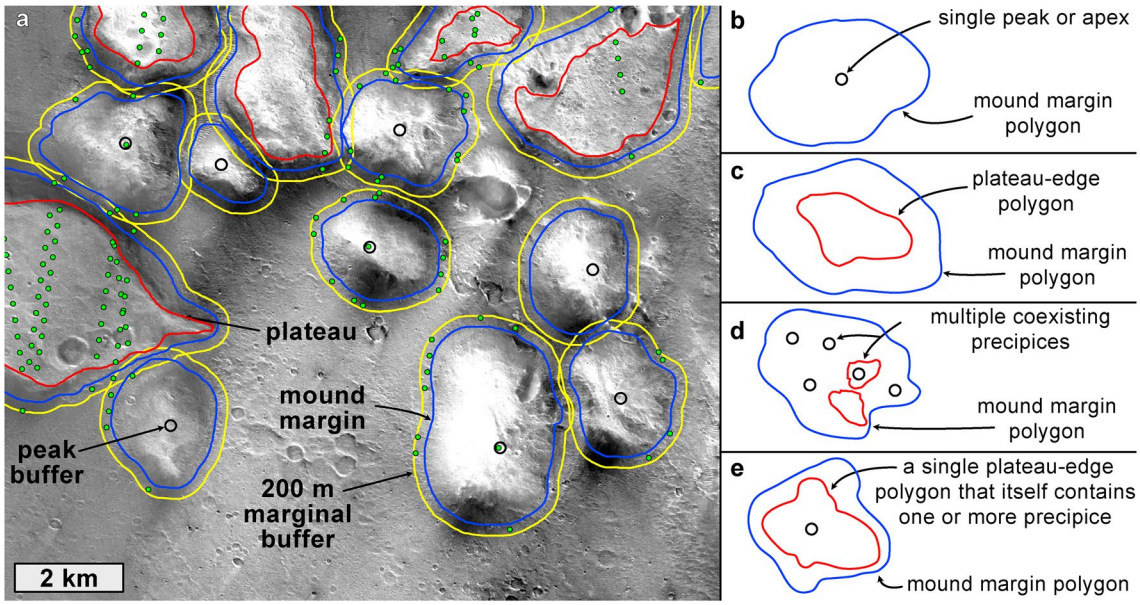

Figure 2. (a) Context Camera (CTX) image showing a field of mounds. The margins of individual mounds (blue lines), the edges of plateaus (red lines), and the mound peaks (center of small black circles) have been digitised by hand. 200 m diameter buffers (yellow lines) have been created around the margins and 100 m radius circular buffers (black circles) have been created around the peaks, in order to capture the relief of the surrounding terrain, and allow for error in the selection of peak locations, respectively. Individual MOLA point data are shown as green points. Mounds that have at least one MOLA datum in its peak/plateau and mound margin can have their heights measured. (b–e) Four examples of how polygon and point data interact in this study, leading to the classification scheme in Section 5.

4.1. Mound Digitization

Mound margins and prominences were digitised manually. Mound margins were digitised as polygons that demarcate the boundary of a mound with the surrounding plains, and wholly enclose the upstanding feature. Prominences were identified from visual inspection of each mound in CTX and HRSC images. Prominences were classified as either peaks (well-defined apexes that can be either smooth or sharp in form, digitised as point features) or plateaus (flat regions at the tops of mounds, where a true apex is missing or indistinct, digitised as polygon features). For each mound, the margin, as well as the number and type of prominences, was recorded by the following convention: (1) a mound with a single peak (one margin polygon enclosing one peak, Figure 2b); (2) a mound with a single plateau (one margin polygon enclosing one plateau polygon, Figure 2c); (3) a mound with multiple peaks or plateaus (one margin polygon enclosing multiple points and/or multiple plateau polygons, Figures 2d); (4) mounds with a single plateau that themselves contain a further distinctive peak (one margin polygon enclosing a plateau polygon containing an additional peak, Figure 2e). The results from this digitization convention were then used to develop the morphological classification explained in Section 5.1. Clusters of mounds that form distinctive arcuate populations that cover >60° of a full circle were digitised using the CraterTools add-in for ArcGIS 10.1 (Kneissl et al., 2011).

4.2. Elevation Data

To investigate the mound morphometry, we used the digitised margins and prominences to extract elevation information from the MOLA and HRSC datasets. The MOLA point data have better vertical accuracy than HSRC DEMs and therefore, where there was data for the mound base and peak, they were used in preference. However, as this only allows for the measurement of ~16% of the mounds, the mounds were also measured using HRSC DEM pixels. To calculate the heights of the mounds, we subtracted the elevation at the base of the mound from the maximum elevation of the mound prominence. In order to extract the elevation at the base and prominence, a 200 m buffer was constructed around the mound margin, and a 100 m radius buffer was constructed around each peak (Figure 2a). A 200 m margin buffer was selected as it is large enough that sufficient MOLA points should fall within the buffer for the average measurement

to be representative of the plains, and small enough that it mitigates the impact of proximal topographic features (i.e., other mounds, craters) on the final plains measurement. The same is true for the 100 m radius peak buffers; their diameters are large enough to collect a single MOLA shot, if there is one present in that location, but small enough that they are representative of the true peak. Plateau polygons did not require a buffer, as they already define the maximum extent of the upper surface of the mound. From these buffers we extracted the mean elevation of pixels from HRSC Digital Terrain Model (DTM) MC-11 quadrangle data (~50 m/pixel, Jaumann et al., 2007; Kersten et al., 2018) and the MOLA PEDR (Point Experimental Data Records; Zuber, 1992) point data that fell within each buffer. In situations where multiple MOLA points or HRSC pixels existed within a marginal plains buffer, the mean topographic value was calculated using both datasets in order to mitigate the effect of topographic relief elements that could alter the measured plains elevation. In all cases, the maximum elevation value was extracted from the prominences. The heights of the mounds could only be calculated through the MOLA method, if individual MOLA points intersected the prominence and the marginal buffer.

MOLA PEDR coverage is global and therefore covers the entire study area, but the HRSC DTM is confined to the MC-11 quadrangle. As such, HRSC covers all of Zone 1 and Zone 2, but only part of Zone 3, so the heights of 1,780 mounds were not measured using HRSC. Furthermore, the HRSC DTM exhibits significant artifacts in some regions of the study area, so may produce inaccurate mound heights. Due to the irregular local coverage of MOLA points, these data could only be used to determine heights of ~16% of the mounds, however, the mounds that it intersects are spread across the entire region of study, so are representative of the full population. Of the total population of mounds digitised, we were able to extract 2,366 measurements using MOLA (2,151 of which were positive values) and 12,606 measurements using HRSC. 1,939 mounds were measured using both MOLA and HRSC; both datasets are detailed in the supplementary materials. Henceforth, all heights quoted are from the MOLA-derived data, owing to its higher vertical resolution, and substantial number of measured mounds of all sizes that are evenly distributed across all three zones.

5. Observations and Results

5.1. Morphologic Classification

We have classified the mounds into four classes based on the morphology determined by the protocol outlined in 4.1. All four classes have the same basic features: they are pale toned, positive-relief features that are clearly structures independent of the dark plains of Chryse Planitia. The categories are as follows: (1) Hills are isolated mounds that have a single prominent peak or smooth crest (Figure 3a). (2) Mesas are isolated mounds that have a single contiguous plateau with no clear apex at their top, which may be covered by loose material and/or have eroded craters superimposed on it (Figure 3b). (3) Clustered mounds represent mounds that have multiple hill peaks and/or mesa plateaus clustered together, but where the lower elevation areas between the peaks and plateaus do not descend to the elevation of the surrounding plains (Figure 3c). If the lower elevation areas between mounds descend to the level of the surrounding plains, the mounds are classified individually as hills or mesas. Clustered mounds can be further sub-divided into clustered hills (clustered mounds that exclusively contain peaks), clustered mesas (clustered mounds that exclusively contain plateaus), and mixed clusters (clustered mounds that contain both peaks and plateaus). (4) Compound mounds represent multiple landforms that have distinct tiers at different elevations (Figure 3d). The tiers may have distinct individual visual qualities that differentiate them from other tiers in the same mound, or they may appear to be composed of similar material. Further detailed observations of individual mounds are given in Section 5.4.

5.2. Mound Distributions

The population of mounds in this study area forms an arcuate distribution around the southern margin of Chryse Planitia across an area of ~550,000 km^2 between 10°N–28°N and 309°E–342°E (Figure 4). The bases of the mounds occur between elevations of ~−1,800 m and −4,050 m, a total range of 2,250 m. The western section of the study zone, Zone 3, is elevated by >500 m relative to relative to Zones 1 and 2. It is therefore prudent to compare elevation ranges only within the three subsections of the study area. The elevation

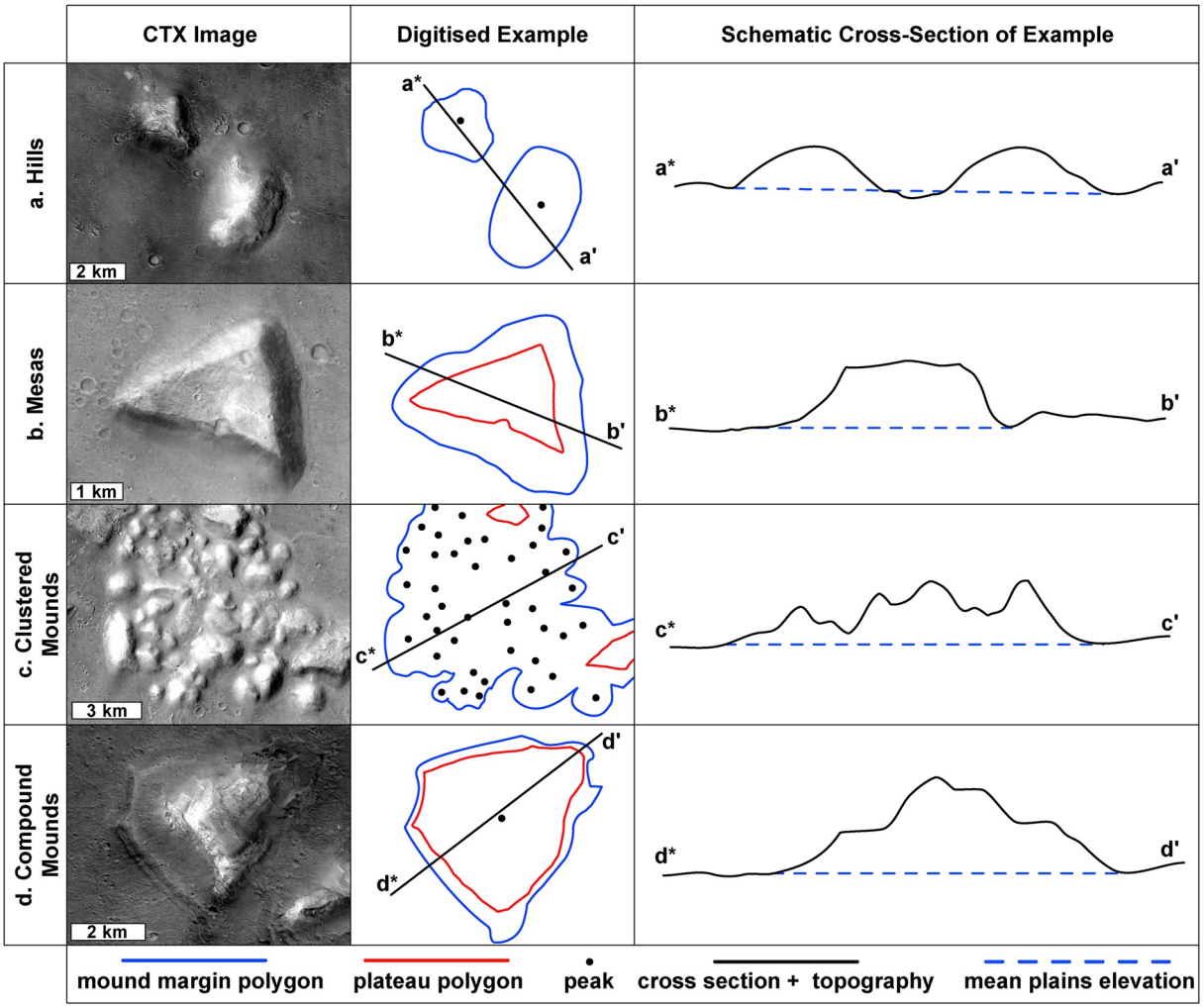

Figure 3. Classes of mounds found in the study area as shown in Context Camera (CTX) data, alongside their digitised forms and schematic cross-sections (a) hills (e.g., 21.997°N, 26.664°W) are rounded features with one apex; (b) mesas (e.g., 19.146°N, 27.505°W), are mounds with one flat-topped plateau area; (c) clustered mounds (e.g., 18.386°N, 28.149°W), contain multiple peaks or plateaus; and (d) compound mounds (e.g., 26.204°N, 24.953°W) contain peaks and plateaus that overlap.

range over which the base of the mounds occur is ~1,550 m for Zone 1, 780 m for Zone 2, and 1,450 m for Zone 3.

The distribution of mounds within the study area appears to be approximately random, however, some mounds occur in curvilinear arrangements or even arcuate patterns (Figure 5). The simplest explanation for this distribution is that they demarcate underlying impact craters. Following this assumption, in cases where mound populations have a circular configuration, we can measure the radius of curvature of this pattern to infer the diameter of the associated impact structure. In the case of a series of mounds forming an incomplete arc of a circle, we have assumed this again delineates a buried impact structure if the mounds occur over more than 60°of arc and the diameter of the inferred impact structures can again be calculated. We located 101 circular or arcuate clusters of mounds that we interpret as indicating buried impact crater structures ranging in diameter from 7 to 143 km (table in supplementary materials). Other groups of mounds cluster proximally to linear and curvilinear ridges that occur within the dark plains material (Figure 5d).

Mesas and compound mounds are common near the dichotomy boundary west and northwest of McLaughlin crater, and are interpreted to be erosional sections of the plateau in this region. The mesas and compound mounds in this location grade into smaller mesas, clustered mounds, and hills.

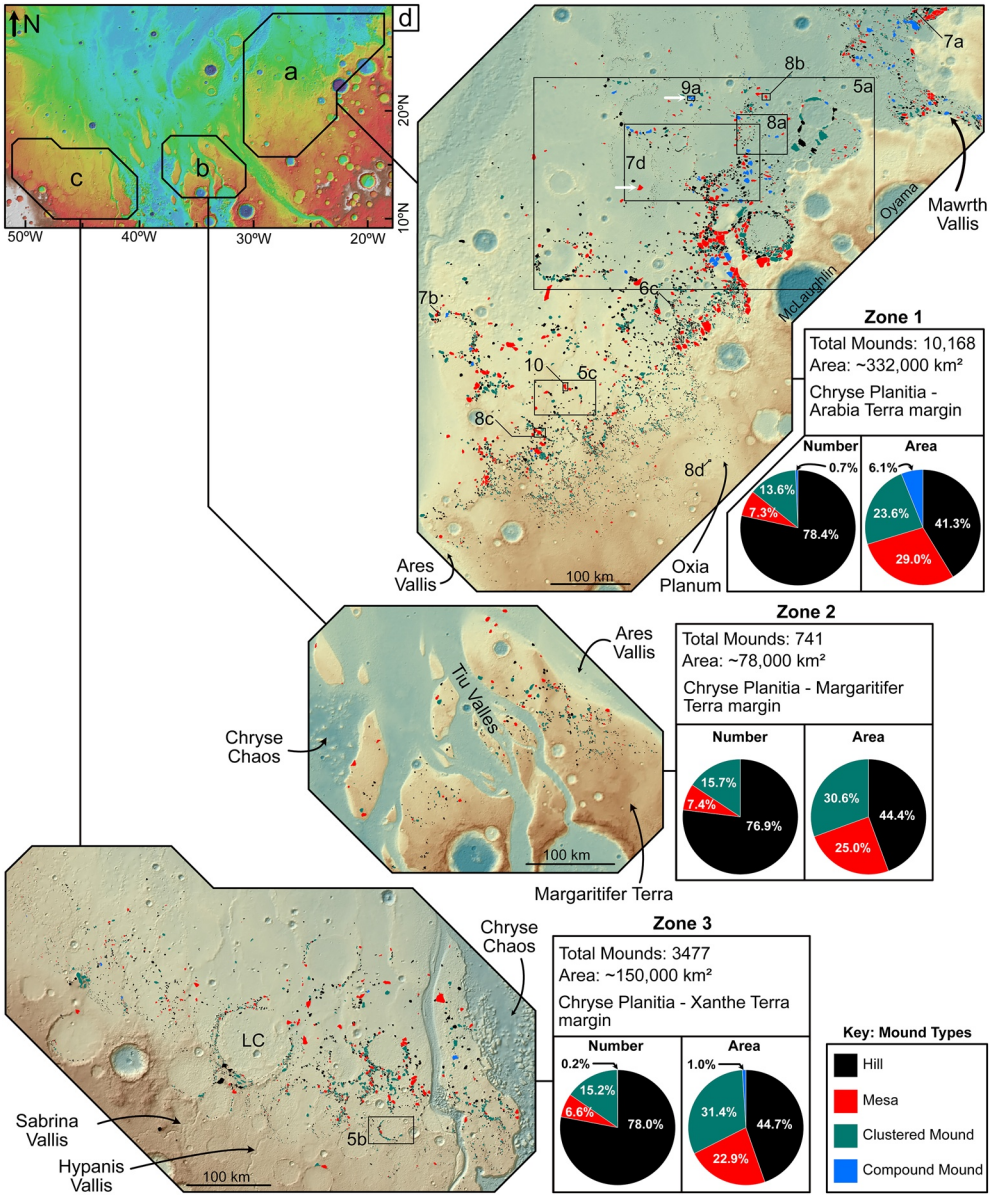

Figure 4. The distribution of mounds (hills: black, mesas: red; clustered mounds: green; compound mounds: blue) within the substudy areas. (a–c) denotes Zones 1–3 respectively, as HRSC-MOLA blend shades (Zones 1–2) and a MOLA blend shade (Zone 3). LC: Lederberg Crater. The percentages of mounds that make up the populations in each subarea are shown as two pie charts; "Number" shows each class as a percentage of the population by number, and "Area" shows the classes as proportions of the total area of the mounds in the subarea. (d) MOLA map of southern Chryse Planitia showing the locations of the sub-study areas. All other numbers and rectangles indicate the position of other figures. The white arrows indicate the location of CRISM observations of mounds containing hydroxylated silicates and sulfates for a compound mound in Figure 4a, box 9 and a mesa in Figure 4a, box 7d. HRSC, high resolution stereo camera; MOLA, Mars orbital laser altimeter.

5.3. Mound Morphometry

We used topographic data in tandem with the digitised mound data set to calculate the heights of the different classes of mounds above the surrounding plains of Chryse Planitia (Table 1). Using MOLA-derived measurements, we calculated that hills have the lowest mean height at ~65 m, followed by clustered mounds (~104 m mean height), mesas (~168 m mean height), and compound mounds (~219 m mean height). The clustered mound subsets of clustered hills, mixed clusters, and clustered mesas have mean

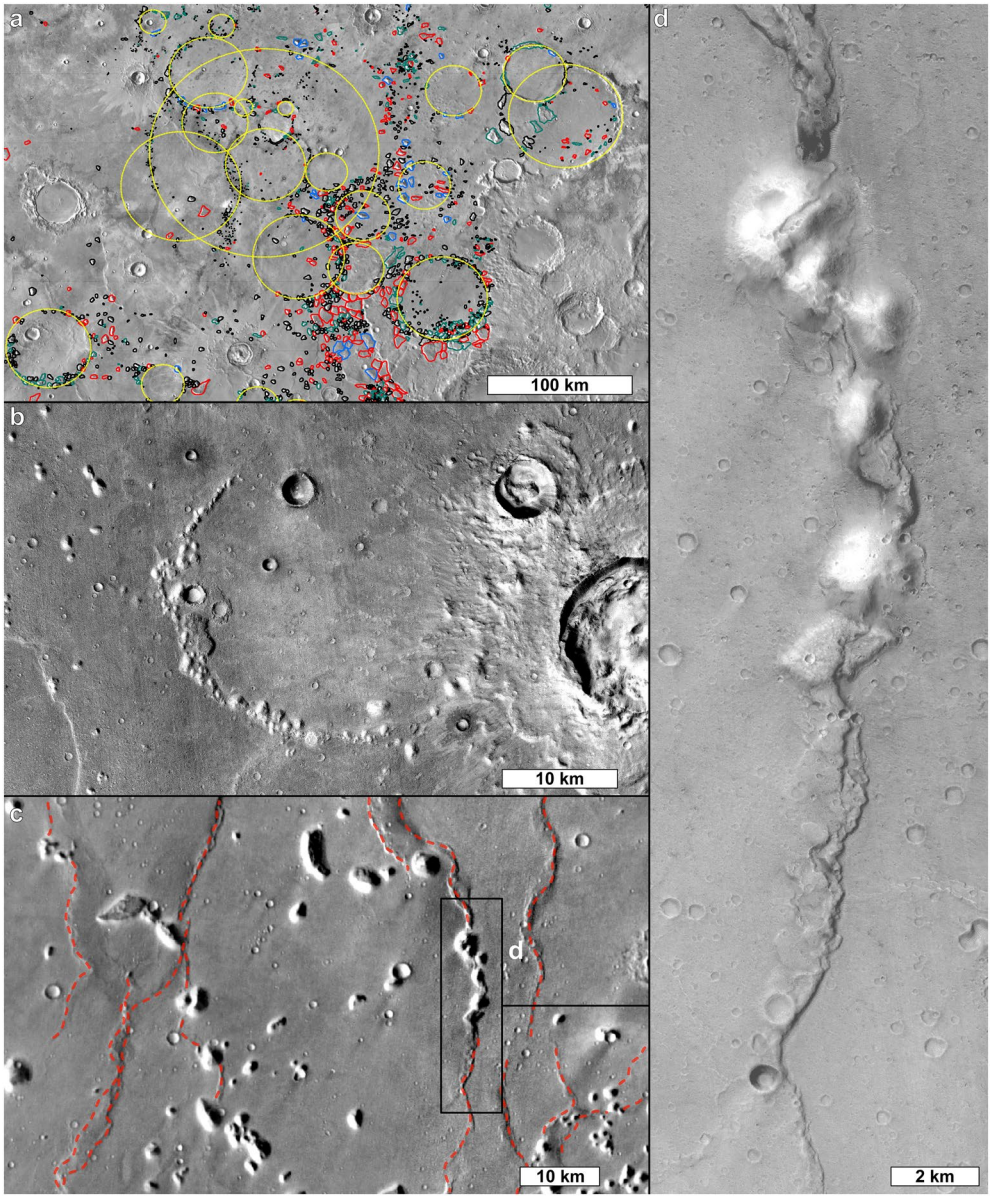

Figure 5. (a) night-time infrared Thermal Emission Imaging System (THEMIS) image showing the northern section of Zone 1, where populations of mounds demarcate the edges of proposed buried impact craters (yellow lines). The largest yellow circle is 143 km in diameter and the smallest (lying within the area of the larger crater) is 7 km in diameter. (b) Context Camera (CTX) image showing a semi-circular population of mounds in Zone 3 (11.308°N, 43.228°W). (c) Nighttime infrared THEMIS image of a mound field in Oxia Planum, showing north-south trending ridges (red dotted lines) that cut through the surrounding material. (d) CTX image showing a population of mounds that follow a north-south trending ridge (19.637°N, 27.329°W).

heights of ~81 m, ~190 m, and ~230 m respectively. The areal extents of the mounds varies with their morphologies, but follows the same trend as the heights: hills are the least extensive with a mean area of <1 km^2, followed by clustered mounds (~3 km^2), mesas (~6 km^2), and compound mounds (~15 km^2, Table 1). We calculate that in general the heights of the mounds increase with areal extent, upto a maximum of ~500 m, corresponding to a surface area of ~ 10 km^2, after which the height does not increase further (Figure 6a). Using the HRSC DTM, the same height-area trend is observed. Most mounds are small, with only 10% of the population being above a height of ~238 m. Our data also highlight the propensity for class populations to be more prevalent at particular heights: most mounds below a height of ~150 m are hills or clustered mounds, but above ~150 m, most mounds are either mesas or compound mounds (Figure 6b).

Table 1
Table Summarizing the Morphometric Features of the Mounds in This Study, Derived From Mars Orbital Laser Altimeter (MOLA) Point Data

		Hills	Mesas	Clustered mounds	Compound mounds
	Number of examples	11,255	1,029	2,025	77
Population	% (by number)	78.24	7.15	14.08	0.54
	% (by area)	42.13	27.58	25.53	4.76
Height (m)	Mean	64.7	167.9	104.1	219.3
	Median	37.3	141.3	65.6	172.6
	Minimum	≪1	3	<1	40.8
	Maximum	453.6	500.5	453.3	593.8
	IQR	62.96	177.01	122.14	165.80
Area (km^2)	Mean	0.9	6.41	3.02	14.78
	Median	0.28	3.31	1.26	10.47
	Minimum	0.01	0.1	0.03	1.3
	Maximum	16.2	131.6	94.6	114.8
	IQR	0.77	6.25	2.89	11.76

Most of the ~500 m tall mounds are mesas or compound mounds, and occur almost exclusively in Zone 1 in the region proximal to Mawrth Vallis (Table S1).

5.4. Mound Characteristics and Stratigraphy

This section outlines the observations of geological features that are common throughout the general mound population, as well as specific examples at HiRISE-scale. The stratigraphic relationships between the dark plains material and the clay-bearing plains of Oxia Planum are also discussed.

The mounds are pale-toned features that contrast with the surrounding dark plains in visible images and that are dark in nighttime THEMIS infrared images, indicative of low thermal inertia on the scale of 100 m. Rarely, some mounds are moderately bright in night-time THEMIS infrared images, suggesting that these bright mounds at least are coarse-grained or indurated sedimentary deposits, or are areas of exposed bedrock (Fergason et al., 2006). Layering can be seen on the flanks of several mounds across the study area (Figures 7a and 7c). As most mounds appear to be covered in loose material, it is unclear what proportion of mounds are layered. However, ~40 mounds in the northern region of Zone 1 exhibit a distinctive, decameter-thick pale-toned layer that is visible in CTX images (Figures 7d–7g). This layer occurs in mounds that are distributed over an area of ~8,000 km^2. The pale-toned layer occurs in mounds that demarcate a large buried crater, suggesting the mounds are not part of the crater rim. Mounds that occur within buried craters at similar topographic heights also contain the same layer, suggesting that the mounds are not a rim feature. Many mounds also have bright rings of extremely pale toned, high albedo material associated with them (Figure 7b) that is similar to the deposits seen around craters and postulated hydrothermal "mega-vents" in Meridiani Planum and Aram Chaos (e.g., Hynek et al., 2002; Ormö et al., 2004).

The relationship of the mounds with the dark plains material is often ambiguous due to the scree that mantles the mound margins. Despite this, individual examples of mounds show evidence of being embayed and buried by the dark plains material (Figures 8a, 8c and 8e), suggesting that, in general, the mounds pre-date the dark plains material. A clear contact between a mound and the clay-bearing unit of Oxia Planum is observed (Figure 8f), showing that the mounds post-date the clay-bearing unit, which is in agreement with the interpretation in Quantin-Nataf et al. (2021).

Mounds that are proximal to Mawrth Vallis commonly contain meter to decameter-scale layering in their upper flanks (Figure 9). In HiRISE IRB images, the hue of the strata ranges from pink to white to blue (Figure 9d), and the lateral continuity of strata can be observed for upwards of 2 km. Where these layered

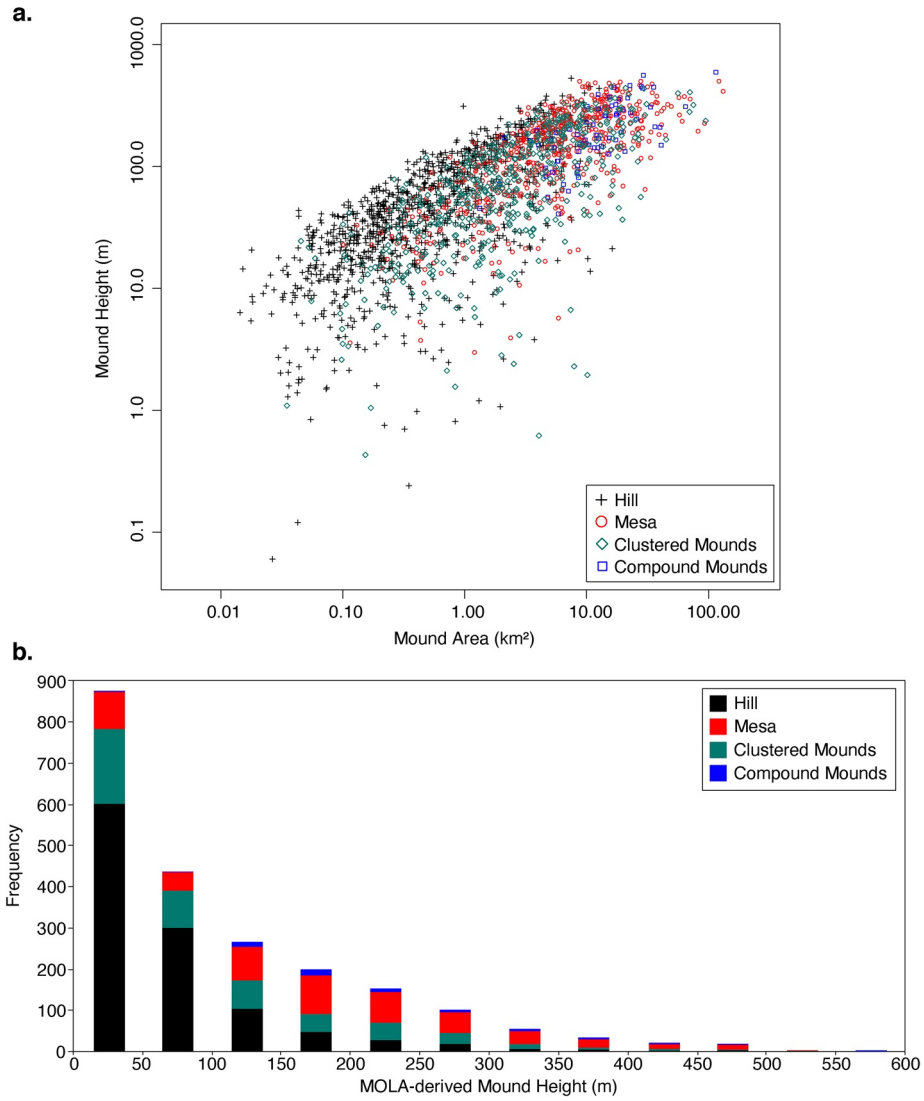

Figure 6. Graphs displaying information about the morphometrics of mounds. (a) The relationship between height and area for 2,151 mounds of different classes, derived from individual MOLA shots at 300 m spacing. Note the propensity for hills to be small, clustered mounds to be intermediate, and mesas/compound mounds to be large, with the tallest and largest examples (>10 km^2) being a consistent ~500 m in height. (b) A size-frequency plot of 2,151 mound heights showing that most mounds are small (50% of the measured population are >68 m in height), and that most mounds below ~150 m in height are hills or clustered mounds, and most mounds above ~150 m in height are mesas or compound mounds. MOLA, Mars orbital laser altimeter.

materials are exposed, they do not preserve impact craters as well as the surrounding, darker material. The layered sections contain dark negative relief lineaments, interpreted as fractures filled with loose material, positive relief lineaments, interpreted as fractures infilled with resistant material, and evidence of faulting, with displacements of up to tens of meters. Although largely obscured, some material that is pale toned and stratified can be seen in the lower tiers as well. The layered material is overlain by a darker, crater-retaining layer that is tens of meters thick, which is comparable to the dark capping unit (e.g., Loizeau et al., 2012) that overlies similar layered material in Mawrth Vallis. The fractures in the layered material do not appear to pervade into the overlying dark capping unit, but the faulting clearly displaces the dark capping unit in some mounds (Figure 9d). The dark capping unit appears to be draped disconformably over the mounds that contain the layered material.

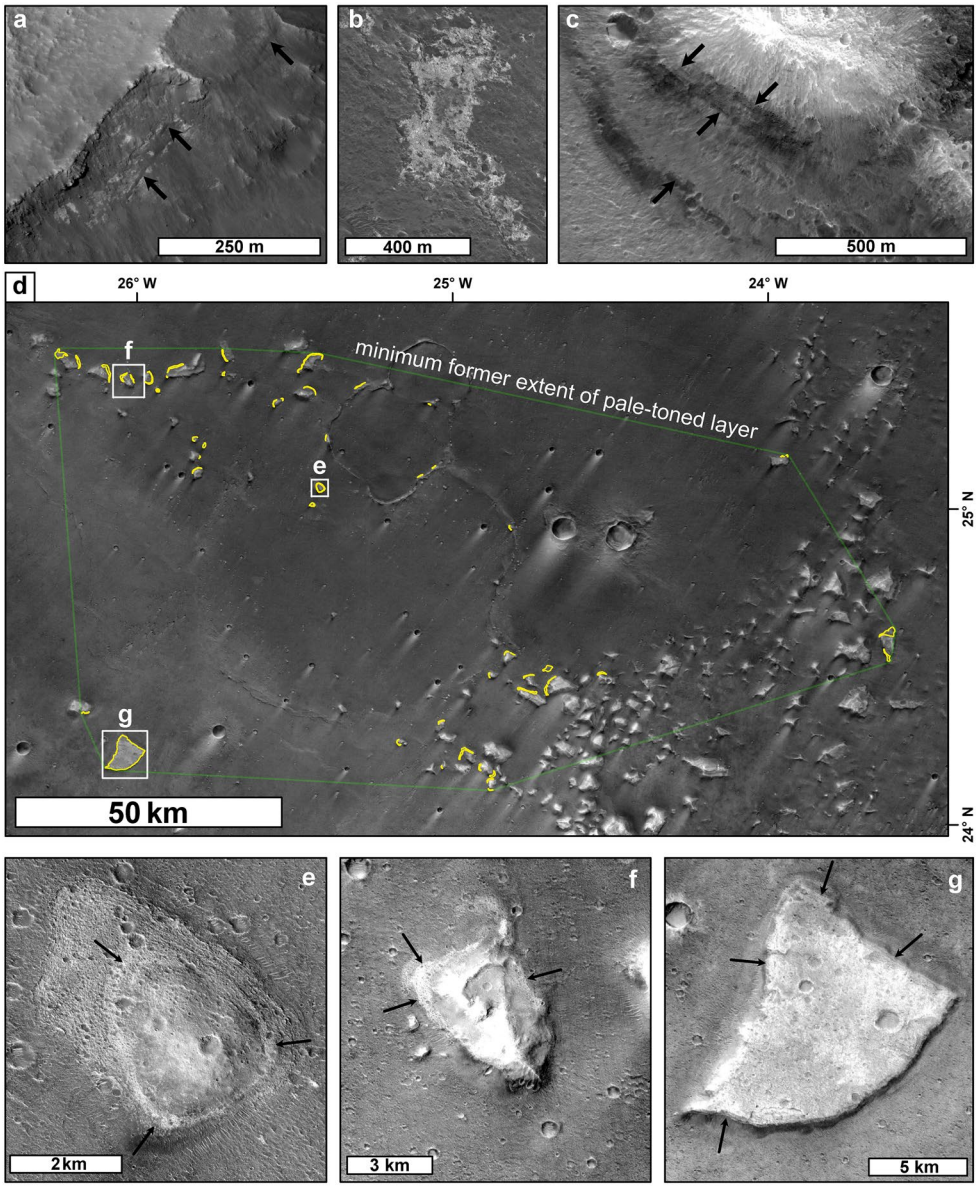

Figure 7. (a) Layering in the flanks of a mesa near Mawrth Vallis, including a thick dark layer (arrowed) partially obscured by loose material (High Resolution Imaging Science Experiment [HiRISE] ESP_036160_2065). (b) Example of pale-toned material that occurs preferentially around mounds and tectonic features that appears to be overlain by the dark plains material (HiRISE ESP_046710_2015). (c) Partly obscured layering (arrowed) in the flanks of a mound north of Mawrth Vallis (HiRISE ESP_044402_2020). (d) Context Camera (CTX) mosaic showing the locations of pale-toned layers identified in the flanks and tops of mounds (yellow margins) and minimum bounding extent if this were once a continuous layer. (e) Mound containing a pale-toned horizontal layer (black arrows). The dark plains material abuts and onlaps the edges of the paler material (HiRISE ESP_064749_2055) (e) CTX image showing pale-toned layer (black arrows) that occurs in mounds demarcating a large (~50 km diameter) crater, suggesting that the mounds are not part of the crater rim, but were originally contiguously on top of the crater margin. (f) CTX mosaic showing a mesa with resistant pale-toned upper "cap rock" layer (margins shown by black arrows).

Similar pale-toned layered material is observable in a HiRISE image of a mound that lies 400 km south-south-west of the mound in Figure 9 and 500 km from the same material found in mounds in the mouth of Mawrth Vallis (Figure 10a). The pale-toned areas of the mound contain a network of dark to pale-brown curvilinear decameter-width bands with a variety of surface relief types that sometimes form polygonal arrangements

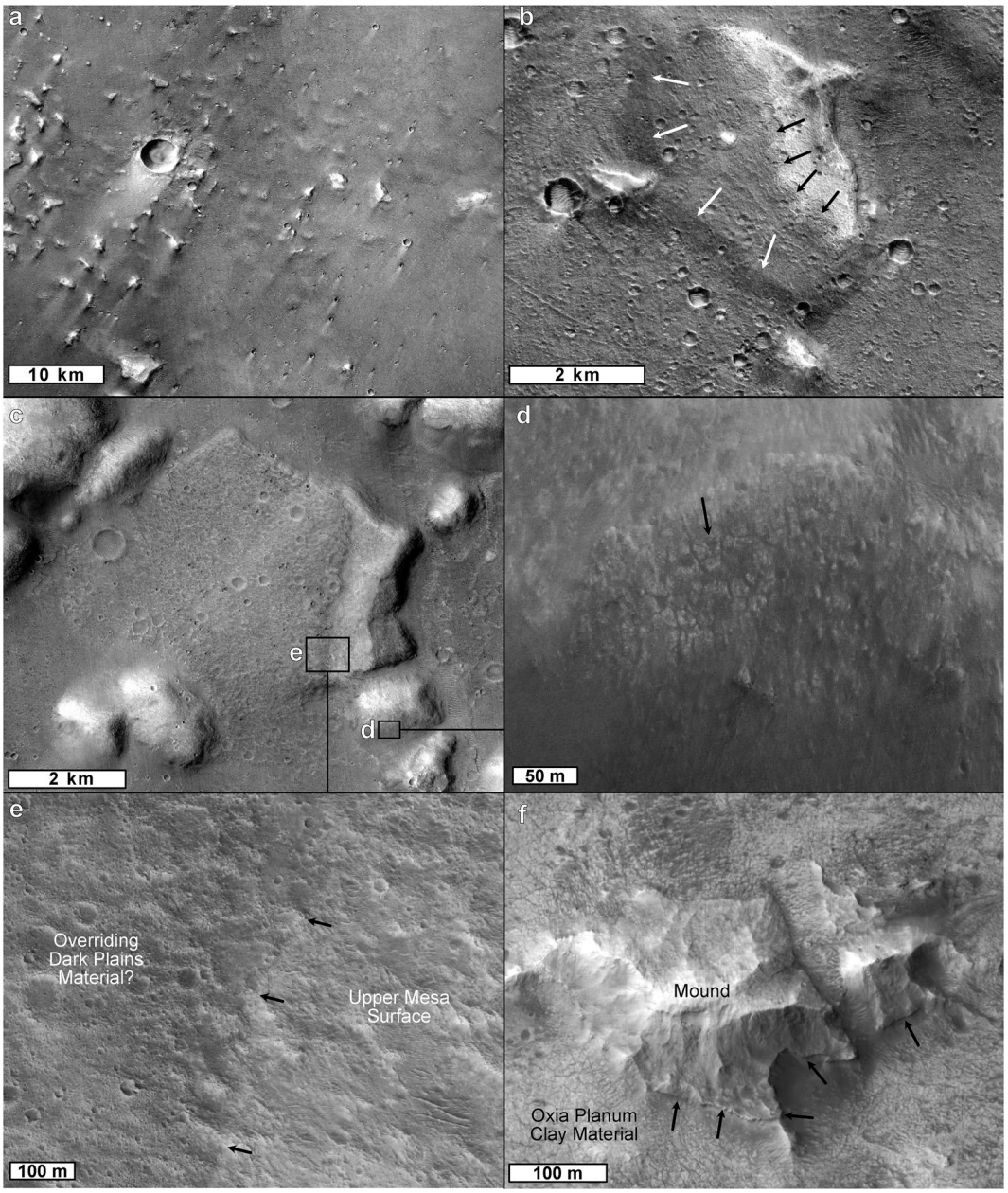

Figure 8. Examples of the stratigraphic relationships of mounds across the study area. (a) Context Camera (CTX) image (mosaic: P21_009247_2056_XN_25N023W, B21_017884_2046_XN_24N023W, G03_019585_2043_XN_24N023W) showing a field of pale toned, high-relief mounds (west and center east), as well as darker, low-relief mounds that appear to be buried by the surrounding dark plains material of Chryse Planitia. (b) Pale-toned mound with arcuate embayments at the edge of its exposed top, as well as a smooth scarp (white arrows) interpreted as the true edge of the underlying mound that is buried by the dark plains material (High Resolution Imaging Science Experiment [HiRISE] ESP _065316_2065). (c) CTX image G19_025730_1977_XN_17N028W showing a mesa and surrounding mounds in the Oxia Colles region. (d) Decameter scale polygonal structures (black arrow) in the flanks of a hill (HiRISE ESP_ 065857_1990). (e) HiRISE image showing the boundary (black arrows) between the dark-toned material and mesa surface of (c), where the dark material is similar in relief and texture to the dark plains material that surround the mesa (HiRISE ESP_ 065857_1990). (f) Mound in Oxia Planum with a clear lower boundary (black arrows) that superposes the fractured clay material that dominates the area (HiRISE PSP_009880_1985).

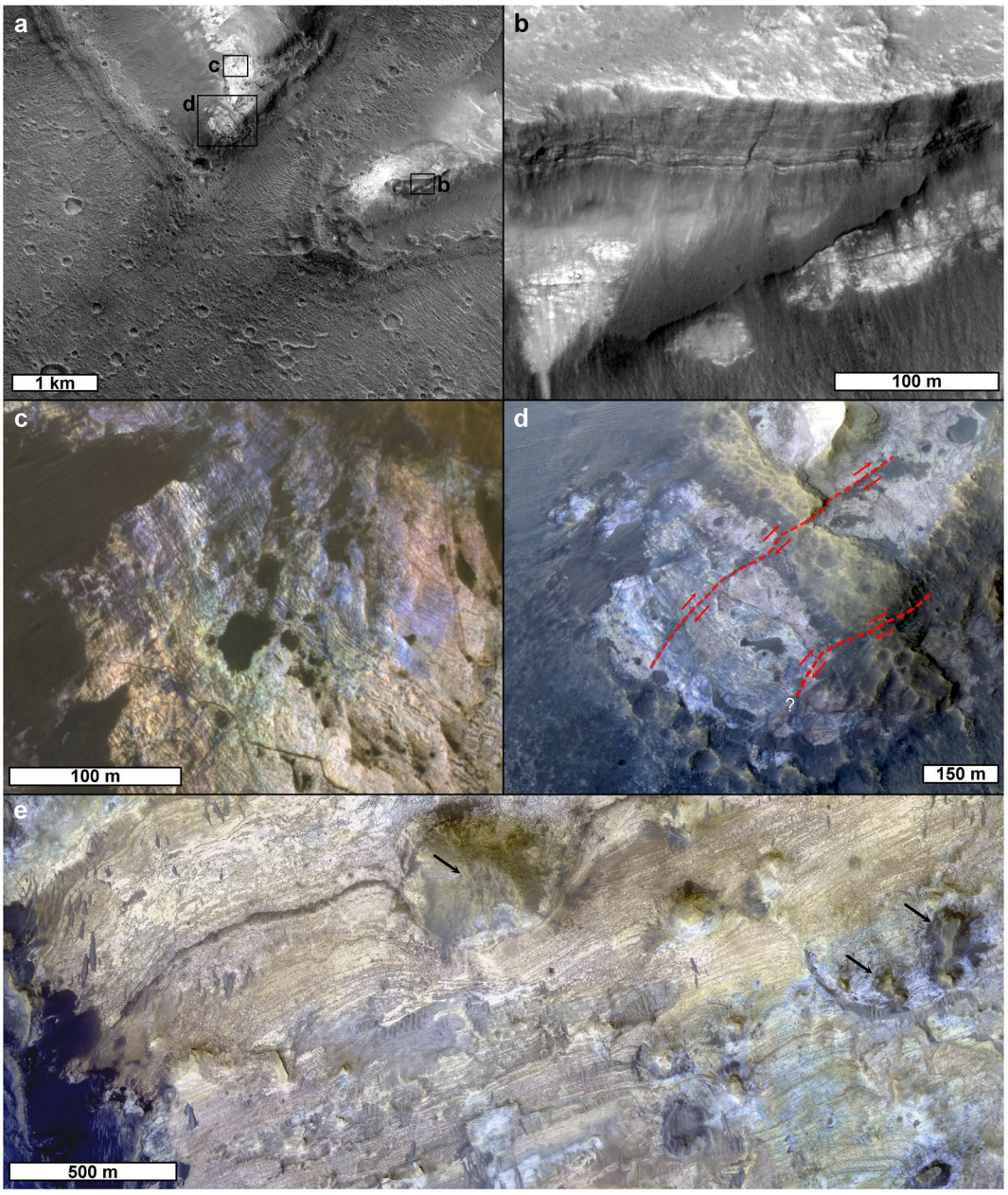

Figure 9. Examples of Mawrth-like strata in a pair of compound mounds that lie ~285 km from the mouth of Mawrth Vallis, as well as an image showing representative strata in Mawrth Vallis as a comparison. (a) Overview of the mounds (High Resolution Imaging Science Experiment [HiRISE] image ESP_063259_2065) showing the location of parts (b–d). (b) Laterally extensive decameter-scale layering in a cliff-face at the top of the eastern mound, which is overlying pale-toned layered material (HiRISE image ESP_063259_2065). (c) Subdecameter-scale layers in the flanks of the western mound (IRB HiRISE image ESP_063905_2065, contrast enhanced to show layering and color variation). (d) Color image of layers at the base of the upper tier of the western mound. The layers range from blue to black-and-white to pink in tone, and are capped disconformably by the brown dark capping unit. All of these units are crossed by a NE-SW trending fault (red dotted line, central) that has displaced them by ~100 m. The relative direction of movement along the fault is shown by arrows. Another potential fault is visible ~300 m to the south east (IRB HiRISE image ESP_063259_2065). (e) Representative section of exposed clay-bearing strata at Mawrth Vallis, showing its similarity to the layering seen in some mounds. The strata are capped by isolated patches of material (arrows) that are visually similar to the brown dark capping observed on the mounds (IRB HiRISE image ESP_018530_2045).

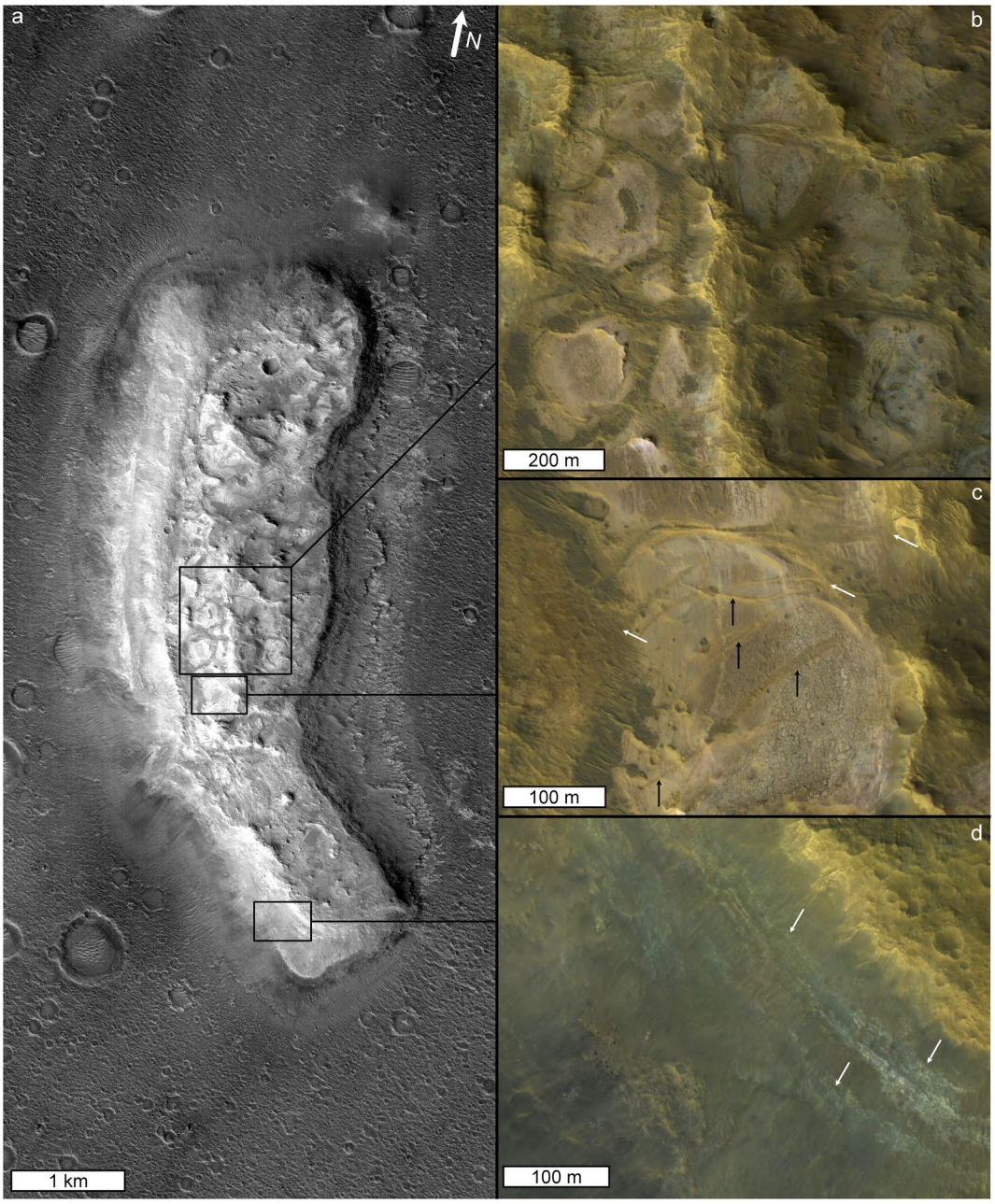

Figure 10. High Resolution Imaging Science Experiment [HiRISE] image of a mound in Oxia Colles (image center at 19.883°N, 27.669°W; IRB HiRISE ESP_066622_2200), showing (a) the overall mound morphology and relative position of parts (b–d). (b) Dark curvilinear bands that cut through the pale-toned bedrock, sometimes forming enclosed segments (bottom left). (c) Area of polygonally fractured pale-toned bedrock crosscut by curvilinear fractures or lineaments (black arrows), that disappear at the margin of the overlying dark-toned units (white arrows). (d) Layered pale-toned materials on the flanks of the mound (white arrows) that resemble the material in the mounds near Mawrth Vallis (e.g., Figure 9e).

(Figure 10b). As with the fractures in the pale-toned mound material in Figure 9, these bands are truncated by the dark capping unit, as described in Mawrth Vallis by Loizeau et al. (2012).

6. Discussion

6.1. Morphology and Morphometry

The similarity of the tone, layering, and thermal inertia of the mounds examined suggest that they are all composed of similar rock types. Based on this assumption, we interpret the morphology and morphometry of individual mounds to primarily be an expression of the amount of erosion. Thus, the typically small and rounded hills imply a high degree of erosion and a late stage of escarpment retreat, whereas the more aerially extensive mesas with flat tops and angular sides suggest a lesser amount of erosion and escarpment retreat. This is also supported by the observation that, in general, mesas and compound mounds are closer to the dichotomy boundary (Figure 5c) and hills are further away, although the presence of overlying impact ejecta often obscures this fact (e.g., Figure 4a). Smaller mounds are seen to grade into the larger dichotomy-proximal mesas and plateaus, again suggesting that the smaller mounds represent the degraded former extent of the mesas, and were once part of a more continuous structure, such as a contiguous layer (or layers) of material, before erosion took place (e.g., Figure 5c). Figure 6 shows that hills are generally smaller features (in both height and area) than mesas. This supports the interpretation that hills have undergone a higher degree of erosion than the mesas. Alternatively, mesas may be mechanically more competent than hills; That is, they may have an additional protective upper layer that hills do not, or may be indurated to a higher degree.

Mesas and compound mounds are the tallest mound type. Clustered mounds are intermediate in both morphology and height, suggesting that they represent a transitional erosional state between hills and mesas. Importantly, Figure 6a shows that height does not increase linearly with area, but reaches a maximum of about 500 m. The fact that mesas (assumed to be amongst the least eroded mounds) conform to this 500 m ceiling suggests that this height limit is not one imposed by erosion, but is instead representative of a minimum original upper thickness of the material that forms the mounds. It is not possible to estimate the maximum upper thickness because the base of the mounds is obscured by the post erosional embayment of the dark plains material (the thickness of which is not known).

The prevalence of each mound class also provides an indication of the erosional state of the entire population. Most of the mounds are hills (78.2% by number, 42.1% of the combined mound area), a few are clustered mounds (14.1% by number, 25.5% of the combined mound area), and still fewer are mesas (7.2% by number, 27.6% of the combined mound area). The large proportion of mounds that are hills, assuming all the mounds are of similar composition, suggest that the population as a whole is in an advanced erosional state. It is unclear why some mounds are more eroded than others, but it could relate to change in the strength of the eroding mechanisms such as variation in wind strength at different latitudes, differential flow of water in different regions, or to preferential hardening of the mound layer near to the dichotomy boundary.

We conclude that the general correlation of mound height and class, the minimum 500 m height limit across the whole mound population, the greater proportion of hills (assuming all mounds are composed of similar rock types) and the distribution of the mounds relative to the dichotomy boundary indicates that the mound population represents the remnants of a highly eroded layer or layers. We have used this as our working hypothesis for the origin of the mound-forming material in the following discussion.

6.2. Mound Distribution

This section focuses on the spatial distribution of the population of mounds as a whole, and also discusses the differences between the subpopulations that exist in each zone. As a whole, the population of mounds extends several hundred kilometers into the northern lowlands, implying that the layer(s) the mounds formed from once covered a substantial amount of the northern lowlands proximal to the dichotomy boundary (e.g., Figures 5and 7). Building on our working hypothesis that the mounds were previously connected as part of a contiguous layer (or layers) in the Noachian, and that they exist at the Oxia Planum ExoMars landing site, we further suggest that the mound-forming layer superposed the Early Noachian clay-bearing unit present here (Quantin-Nataf et al., 2021).

As the bases of the mounds in Zones 1 and 3 have very similar relative elevation ranges of 1,500 m, this also suggests that they are likely to have been originally the same layer within the regional Chryse Planitia stratigraphy. The similarity of these elevation ranges in the two zones with the largest number of mounds, suggests that the original elevation of the area where the mounds occur was ~1,500 m. Only approximately half of this elevation range is represented in Zone 2, probably owing to substantial erosion on both sides by Ares Valles and the combined Tiu Valles-Chryse Chaos system. The absolute elevation of Zone 3 is greater by >500 m relative to Zones 1 and 2 due to its proximity to the margin of the Tharsis rise. Assuming that the proposed mound forming layer formed at similar elevations around the circum-Chryse region, this suggests that the majority of the uplift of Zone 3 occurred after the mounds were formed from their original layer. Given that the majority of the Tharsis bulge was in place by the end of the Noachian (e.g., Carr & Head, 2010; Phillips et al., 2001; Werner, 2009), it would follow that the mounds were already in place by this time too.

6.3. Preservation of the Mounds

The preferential occurrence of mounds around the edges of buried impact craters and near to tectonic ridges, together with the interpretation that the mounds formed from the erosion of an approximately contiguous layer or set of layers, implies that these areas were more resistant to the erosion that isolated the mounds. To form the circular arrangements of mounds we see today (Figure 11), the preservation process for the mounds must therefore involve selective reinforcement of the hypothesized layer(s) above the edges of impact craters. The most reasonable mechanism for the increased erosional resistance of the mounds is cementation of the strata by resistant minerals precipitated from groundwater. We propose that: (1) the crater-delineating and ridge-proximal mounds overlie regions of relatively more fractured, and therefore more permeable crust that once acted as a conduit for groundwater outflow; (2) mineral precipitation would therefore have preferentially affected the material overlying the fractured locations; and (3) once emplaced in the host layer, the precipitated minerals (e.g., iron oxides, carbonates, or sulfates) would have improved the mechanical competence of these regions, making them more resistant to erosion (e.g., Wagh & Tarrer, 1991; Yasir et al., 2018). Bleaching of material in areas of tectonically controlled hydrothermal fluid flow is observed in Meridiani Planum and Valles Marineris (Ormö et al., 2004; Treiman, 2008), and we suggest that the general pale tones of the mounds might also be partially attributed to this phenomenon. Furthermore, evidence of lineament bleaching is apparent in HiRISE images of an isolated mound that lies 150 km northwest of the ExoMars landing ellipse and 500 km southwest of Mawrth Vallis (Figure 10). We propose that the curvilinear brown bands that cut the pale-toned bedrock in Figure 10 are fractures surrounded by regions of altered or bleached bedrock, where fluid has exploited the fracture and deposited minerals in the surrounding bedrock, changing its tone and resistance to weathering. The alteration zones cut through the pale-toned layered unit, but are themselves truncated by dark capping unit, suggesting the episode of alteration occurred before the dark capping unit was emplaced (at ~3.7 Ga if this is the same material as described in Mawrth Vallis by Loizeau et al., 2012). Alternatively, the mound forming layer may have simply been draped onto the pre-existing topography, and the observed mounds are the highest points of the exposed layer. However, this seems less likely, and no specific evidence to reinforce this hypothesis has been observed.

The large distances (>100 km) between the similar pale-toned meter-scale layering suggest that the original layer may once extended across the whole area, further implying that all the mounds between them were originally part of the same layer. Alternatively, the pale-toned material may have been emplaced in the mound-forming layer from depth by groundwater or hydrothermal processes. Nevertheless, both of these hypotheses require a substantial amount of erosion to have occurred between deposition and alteration of the dark capping unit, in order to remove the majority of the mound-forming layer.

Most of the mounds do not occur in arcuate patterns or near apparent tectonic lineaments. We attribute these mounds to localized fractures in the underlying bedrock that acted as individual conduits for fluid flow, or to buried craters that have had most of their mounds buried or removed through erosion. One possible hypothesis for the randomly distributed mounds is that these mounds occur where a small impact crater impacted on the previously extensive layer inciting enhanced fluid flow and subsequent mineralization; alternatively, the smaller impacts may have occurred earlier and fractured the underlying bedrock prior to

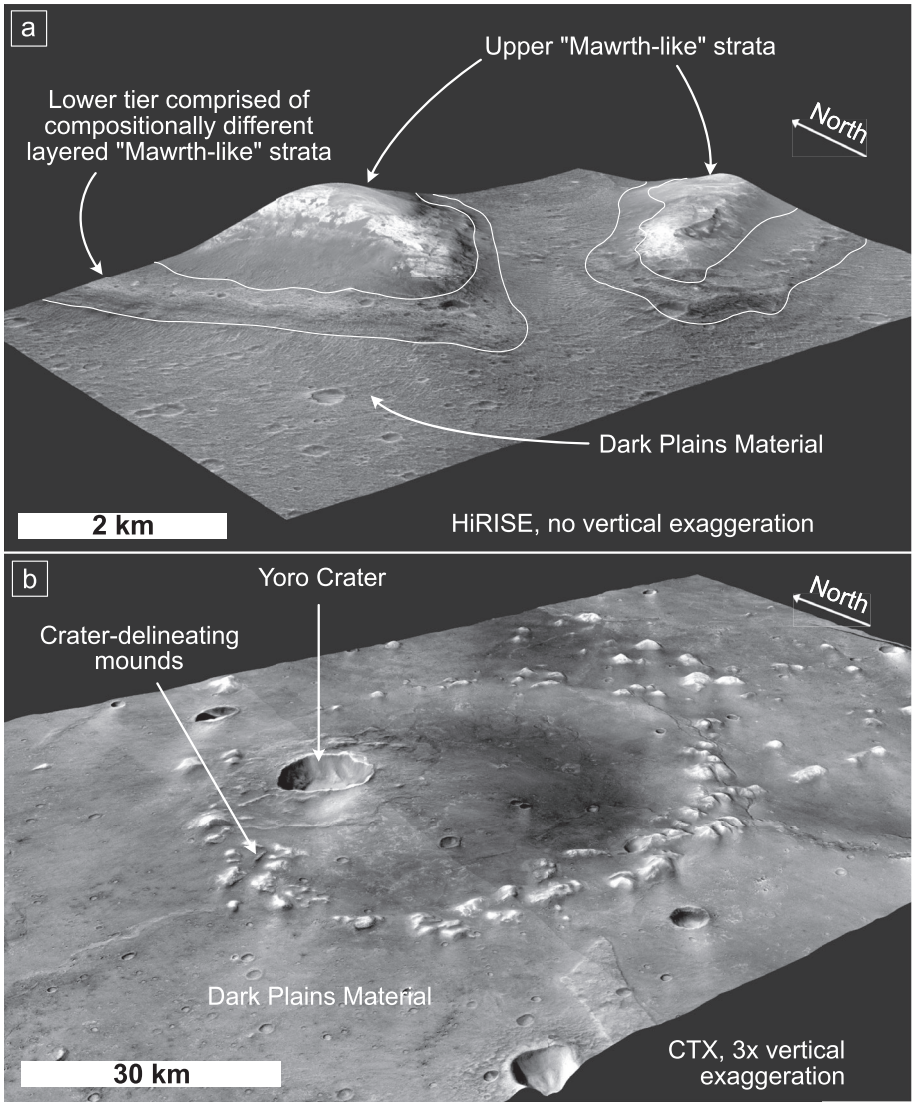

Figure 11. 3D views of (a) the compound mounds explored in Figure 6a (High Resolution Imaging Science Experiment [HiRISE] image: ESP_063259_2065), showing that tiers are traceable between mounds, and (b) crater-delineating mounds (Context Camera [CTX], mosaic image center: 22.616°N, 27.834°W, individual CTX images: D04_028763_2026_XN_22N027W, B19_016948_2010_XN_21N027W, D05_029119_2018_XN_21N027W).

the deposition of the extensive layer. The pale-toned material seen around proposed hydrothermal megavents and crater rims in Ormö et al. (2004) is attributed to fluid flow causing the bleaching of bedrock, or mineral precipitation through the high-permeability margins of impact craters. We attribute the widespread mound-marginal pale-toned material in Figure 7 as being of the same origin, owing to the similar patchy morphology, distributions around fractures, and albedo properties.

Several populations of mounds demarcate small (7 km diameter) to medium (~40 km diameter) craters within a population of mounds that demarcates a very large (143 km diameter) crater (Figure 5a). This suggests that the cratered surface that the arcuate mound patterns represent formed over an extended period of time. This is because the mounds that demarcate these craters lie on the same topographic plane: if the small crater had formed soon after the large crater, it would be within the depression of the larger crater, and therefore topographically much lower. The large crater must have formed first, and was then either significantly eroded so that any new craters that formed within it had their rims at approximately

the height of the eroded rim, or was infilled by post impact detritus almost to the crater rim, before the small crater formed.

The lack of mounds in the intra-crater areas of larger, isolated impact basins suggests that something prevented the intracrater fractures from being effective conduits for the proposed groundwater to percolate and inhibited the superposing material from becoming indurated in these regions. There are two possible reasons why mounds do not regularly form in the center of larger impact craters: (1) crater-fill sediment or impact melt acted as an impermeable layer, prohibiting the induration of material that overlies intracrater areas, or (2) the mounds were able to form in intracrater settings, but where the preexisting topography was lower (i.e., especially on crater floors and in plains regions away from crater rims), most mounds were buried by dark plains material.

It is unlikely that the mounds are the remnants of mud volcanoes because the population lacks any clear evidence for summit craters, as is ubiquitous in other nearby populations interpreted as mud volcanoes (e.g., Brož et al., 2019; Komatsu et al., 2016), and there are no clear observable structures that are associated with flow on the mound flanks. The flat-topped morphologies of mesas seem incompatible with being formed through sedimentary volcanism. It is also unlikely that the mounds represent the edges of buried craters. Although Rodríguez et al. (2007) suggest that many of the mounds are the degraded remnants of impact crater rims, the fact that numerous mounds are shown to superpose the Hypanis delta (Fawdon et al., 2018) in the Xanthe Terra region shows that this cannot be true for all mounds. Similarly, some mounds are found within buried craters, and have similar elevations to mounds outside the crater rim. This suggests that they are not simply remnant crater rim or central peak/peak-ring elements. Furthermore, the pale-toned layer in Figure 7d occurs in both crater-delineating mounds, and extra-crater mounds, suggesting that the mounds are a separate feature from the craters themselves.

6.4. Chronology

In Section 6.2, we used elevation data to propose that the mound-forming layer was deposited or emplaced before the end of the Noachian. Here, we use the stratigraphic relationships we observed in Section 5 to further constrain the timing of the deposition and subsequent erosion of the preexisting layer, to form the mound-like landforms we observe today.

Mounds with clear, regolith-free margins are mantled and embayed by the dark plains material (Figure 8) mapped as the $HNCC_1$ and HCC_2 units in Tanaka et al. (2005). This means that the mounds predate the Late Noachian to Early Hesperian emplacement of these units. This relationship is further shown in Figure 5, where the dark plains material shallowly buries isolated examples of mounds. Furthermore, many mounds are rounded with cove-like embayments on their margins (Figure 8b). The dark plains material clearly onlaps into these embayments, suggesting that the mounds were eroded into their rounded forms before the emplacement of the dark plains material at ~3.55 Ga (Loizeau et al., 2012). In the Oxia Planum region, the mounds directly overlie the Early Noachian (Quantin-Nataf et al., 2021) clay-bearing units, and so must be younger. These stratigraphic relationships provide minimum and maximum bounds for mound formation and show that they are Noachian in age.

Compound mounds offer additional insight into the chronology of events. We propose that the tiering could be a result of compositional or mechanical differences between sections of the stratigraphy, and this might be traceable across different mounds, and even over to the Mawrth Vallis plateau. In particular, the upper levels of some of the compound mounds (Figures 9–11) share morphological similarities with the layered clay-bearing units of Mawrth Vallis (Figure 9e, Loizeau et al., 2012; Michalski et al., 2013; Noe Dobrea et al., 2010) in that they are pale-toned, layered at the meter-scale, and contain hydrated mineral signatures. where there is spectroscopic data available. Layered compound mounds up to 100 km from Mawrth Vallis are suggested in Michalski and Noe Dobrea (2007) to be related to the Mawrth strata, but our analysis shows that the extent of this deposit may have been much greater than previously thought (see Figures 9–11 showing mounds ~295 and ~560 km from Mawrth). Furthermore, our observation that the mound population decreases in height with increasing distance from Mawrth Vallis is consistent with the mound material being reworked or original Mawrth Vallis plateau material, and that those materials thinned with distance

away from the dichotomy. However, as noted in Section 6.1, this could also be attributed to increased erosion with distance from the dichotomy boundary, and may not be associated with the Mawrth region specifically.

The layered upper tiers of some compound mounds contain hydrated minerals (Loizeau et al., 2012; Michalski & Noe Dobrea, 2007) and so originated or were subsequently altered in an environment that supported aqueous hydration of minerals. However, the environment must have become unsuitable for the formation or deposition of hydrated mineralogy prior to the emplacement at ~3.7 Ga (Loizeau et al., 2012) of the Mawrth dark capping unit. This is because that unit contains unaltered igneous minerals and shows no alteration signatures. The Mawrth layered units were emplaced ~3.9 Ga (e.g., Michalski & Noe Dobrea, 2007; Michalski et al., 2010; Loizeau et al., 2012), with subsequent reworking and redeposition occurring within proximal large craters (e.g., Oyama Crater) at ~3.8 Ga (Loizeau et al., 2012). We suggest that the Mawrth-like tiers of compound mounds are an extension of the clay-bearing strata of Mawrth Vallis, or are contemporaneous with the reworked deposits found in Oyama Crater. The compound mounds (e.g., Figure 9) share morphological characteristics (e.g., highly eroded forms, low thermal inertia, pale toned) with the rest of the noncompound mound population. suggesting they have a common origin, which is reinforced by the similar depositional ages determined by their stratigraphic relationships. Hence, the Mawrth-like compound mounds may be genetically equivalent to the wider circum-Chryse mound population. This inference suggests that the wider mound population is older than 3.8 Ga, but younger than the 4.0 Ga lower limit controlled by the age of the Oxia Planum clays (Quantin-Nataf et al., 2021), assuming that, as our data shows, all of the mounds belong to the same population.

The dark capping unit was deposited or emplaced unconformably over the clay-bearing strata of Mawrth Vallis (~3.6 Ga; Loizeau et al., 2012), and was itself significantly eroded before deposition of the dark plains unit of Chryse Planitia (emplaced ~3.6 Ga). This is supported by the observation of a compound mound near Mawrth Vallis (shown in Figure 9), where the dark capping unit truncates the eroded strata of the clay-bearing areas, which are themselves embayed by the younger, unaltered dark plains unit that infills Chryse Planitia.

We propose that a mound-forming layer was deposited or emplaced on the margins of Chryse Planitia between 4.0 Ga and 3.8 Ga (Early-Middle Noachian, Figure 12). The Mawrth-like material that comprises tiered mounds in the Mawrth Vallis area could either represent a separate mound population (and therefore a distinct former layer) or part of the same layer as the rest of the mound population. As the Mawrth Vallis layered unit was emplaced ~3.9 Ga (e.g., Michalski & Noe Dobrea, 2007; Michalski et al., 2010; Loizeau et al., 2012), it is possible that the larger mound population is simply a distal continuation of this material that do not possess the same distinctive layering. Alternatively, they may consist of reworked Mawrth Vallis clay-bearing material that was deposited ~3.8 Ga (Loizeau et al., 2012). Subsequent erosion is then hypothesized to have removed much of this original layer, or layers, leaving the mounds as erosional remnants. These were then partly embayed by Chryse Planitia plains unit materials in the late Noachian to early Hesperian. Importantly, the observation that the mounds superpose the Oxia Planum clays, and may have once been a contiguous part of the same material that forms the Mawrth plateau, suggests that the Oxia Planum clays are older than the Mawrth Vallis clays. An alternative explanation that explains this observation is that the Mawrth-like mounds are a separate younger population, although thus far we have found no observations that specifically support this conclusion.

7. Conclusions

We have investigated the morphology, morphometry and distribution of mounds in Chryse Planitia and conclude that:

- The ~14,500 mounds that were studied in the south Circum-Chryse region can be divided into four classes: hills (isolated, smooth, and round topped), mesas (isolated, flat topped), clustered mounds (groups of nonisolated hills or mesas), and compound mounds (tiered examples). These classes are a reflection of the erosional state of the mounds, mesas, and compound mounds are the least eroded examples, clustered mounds are moderately eroded, and hills are the most eroded examples
- The height-area relationship of the mounds has a height maximum of ~500 m. Combined with the observation of the degree of erosion of different mound morphologies, this suggests that the mounds

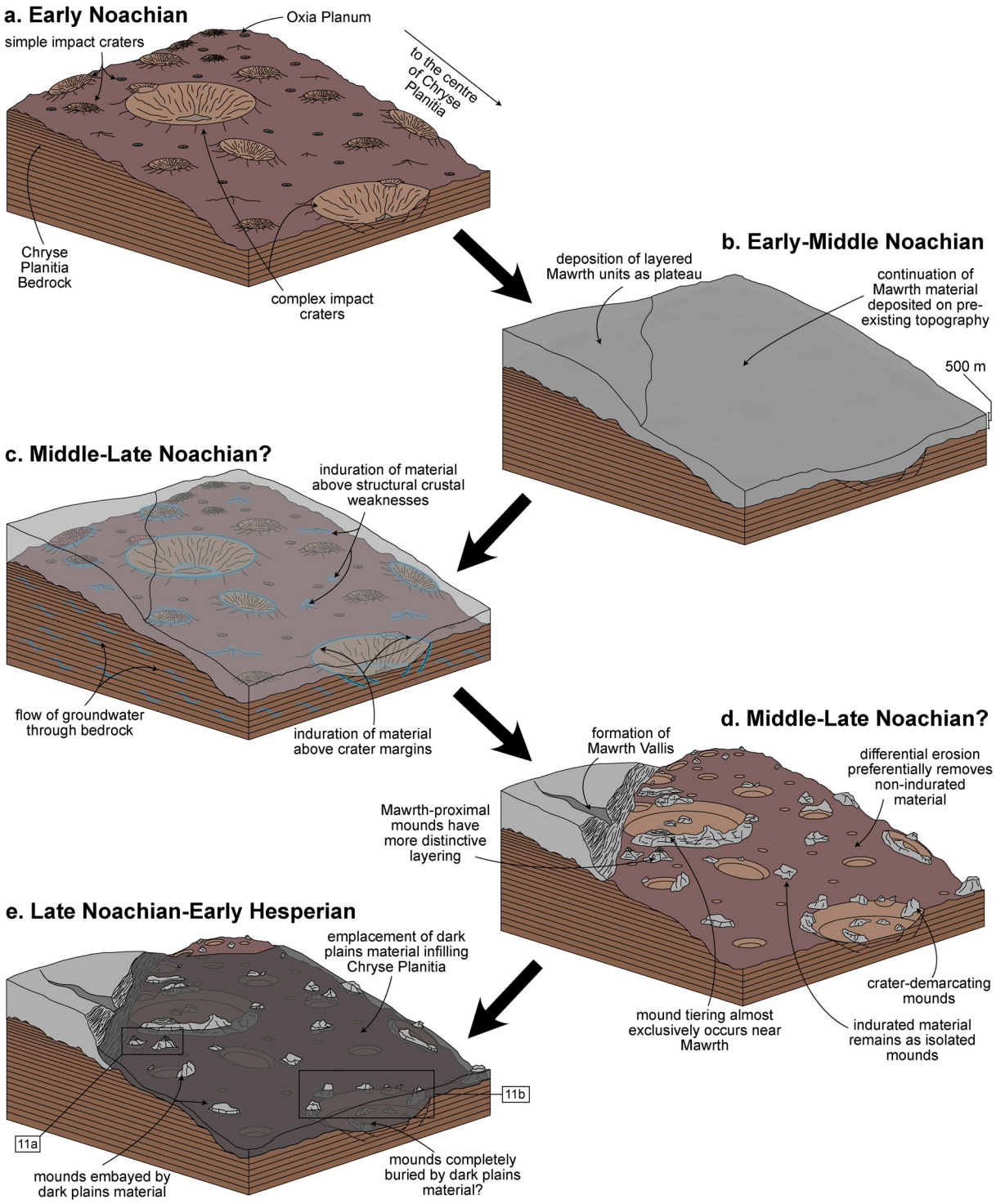

Figure 12. Southward-facing block diagram showing the spatial and temporal evolution of the study area: (a) the topography of the study area post Chryse impact. The extent of the regional layered clay unit that comprises the bedrock of Oxia Planum is unknown, but is here simplified to extend downward into the crust and outwards into Chryse Planitia. (b) >500 m of mound material is deposited or emplaced on top of the regional clay-bearing unit in the Early to Middle Noachian, as well as on the Mawrth Vallis regional plateau. (c) Widespread hydrothermal activity occurs along the dichotomy boundary, indurating material that superimposes crustal weaknesses such as crater-marginal fractures. (d) Erosional processes remove the nonindurated material, leaving the indurated material as remnant upstanding mounds scattered across the topography. (e) Dark plains material is emplaced in the Late Noachian and Early Hesperian, almost entirely mantling the topography, embaying many mounds, and burying some examples.

formed from the erosion of one or more regionally extensive layers that once covered the ExoMars landing site at Oxia Planum, as well as the lowland areas on the margin of southern Chryse Planitia

- The mounds are broadly Noachian in age, and were deposited or emplaced, lithified, subjected to induration by groundwater processes, and eroded between the Early Noachian and Late Noachian. If the meter-scale layering seen in the upper flanks of compounds mounds is analogous to the clay layering seen at Mawrth Vallis, then, assuming the mounds are part of the same population, the mounds probably straddle the Early Noachian-Middle Noachian boundary
- The existence of mounds that contain similar layering to the clay-bearing strata of the Mawrth Vallis plateau suggests that these mounds were once part of a Mawrth-like clay-bearing unit that may have been contiguous with the plateau itself before erosion took place. These mounds appear to belong to the same population as the mounds at Oxia Planum, which overlie the clay-bearing rocks that are the primary target of the ExoMars rover. This suggests that the Mawrth Vallis plateau clays are younger than those in the Oxia Planum region. The Oxia clays could represent a lower part of the regional stratigraphic sequence
- The local distribution of mound-associated buried impact structures supports groundwater processes as part of the preferential preservation mechanism. However, the observation that most mounds form random patterns that are not associated with craters rims, and the presence of several mounds within buried craters argues against the mounds simply being upstanding, embayed, crater rim elements

This study has revealed that the population of isolated mounds in Chryse Planitia are accessible, 3-dimensional exposures of layered Noachian-aged deposits that may have interacted with groundwater. The shape of the mounds, their individual geologic characteristics, and their stratigraphic relationships to one another provide unique insight into a record of the depositional and alteration environments present on early Mars. Our findings emphasise the importance of more detailed studies into their composition and significance with respect to the ExoMars rover landing site in Oxia Planum, and show that, whilst their mode of formation remains somewhat ambiguous, their geological significance is not.

Data Availability Statement

Supplementary information including datasets and additional files for this research are available in McNeil (2021). CTX and HiRISE image data are publicly available at the NASA Planetary Data System repository in the Mars Reconnaissance Orbiter section (https://ode.rsl.wustl.edu/mars/). Tabulated data on individual mound classification, location, and morphometry. Geospatial data vectors (shapefiles, .shp) for mounds. Full-page blow-ups of panels in Figure 4. Additional supporting graphs.

Acknowledgments
J. D. McNeil acknowledges STFC for support under Doctoral Training Grant SA21 5664, and the Open University Space Research Area. M. R. Balme and P. Fawdon acknowledge UK Space Agency Funding: ST/V001965/1 and ST/R001413/1. The authors also thank Susan Conway for her support with HiRISE image ESP_066622_2000, and Susanne P. Schwenzer and Jack Wright for their helpful comments in the early stages of writing. Ranjan Sarkar and an anonymous reviewer and the editor, Deanne Rogers, are thanked for their insightful comments and questions which greatly helped to improve this manuscript.

References

Adler, J. B., Bell III, J. F., Fawdon, P., Davis, J., Warner, N. H., Sefton-Nash, E., & Harrison, T. N. (2019). Hypotheses for the origin of the Hypanis fan-shaped deposit at the edge of the Chryse escarpment, Mars: Is it a delta? *Icarus*, *319*, 885–908. https://doi.org/10.1016/j.icarus.2018.05.021

Brož, P., Hauber, E., van de Burgt, I., Špillar, V., & Michael, G. (2019). Subsurface sediment mobilization in the southern Chryse Planitia on Mars. *Journal of Geophysical Research: Planets*, *124*(3), 703–720. https://doi.org/10.1029/2018JE005868

Carr, M. H., & Head, J. W. (2010). Geologic history of Mars. *Earth and Planetary Science Letters*, *294*, 185–203. https://doi.org/10.1016/j.epsl.2009.06.042

Christensen, P. R., Jakosky, B. M., Kieffer, H. H., Malin, M. C., Mcsween, H. Y., Nealson, K., et al. (2002). The thermal emission imaging system (THEMIS) for the Mars 2001 Odyssey mission. *Space Science Reviews*, *110*, 85–130. https://doi.org/10.1023/B:SPAC.0000021008.16305.94

Duszyński, F., Migoń, P., & Strzelecki, M. C. (2019). Escarpment retreat in sedimentary tablelands and cuesta landscapes: Landforms, mechanisms and patterns. *Earth-Science Reviews*, *196*. https://doi.org/10.1016/j.earscirev.2019.102890

Edgett, K. S., & Malin, M. C. (2002). Martian sedimentary rock stratigraphy: Outcrops and interbedded craters of northwest Sinus Meridiani and southwest Arabia Terra. *Geophysical Research Letters*, *29*. https://doi.org/10.1029/2002gl016515

Fawdon, P., Gupta, S., Davis, J. M., Warner, N. H., Adler, J. B., Balme, M. R., et al. (2018). The Hypanis Valles delta: The last highstand of a sea on early Mars? *Earth and Planetary Science Letters*, *500*, 225–241. https://doi.org/10.1016/j.epsl.2018.07.040

Fawdon, P., Roberts, A. L., & Mirino, M. (2020). Impact crater degradation and the timing of resurfacing events in Oxia Planum. *In 51st lunar and planetary science conference abstract*. Europlanet Science Congress. https://doi.org/10.5194/epsc2020-55

Fergason, R. L., Christensen, P. R., & Kieffer, H. H. (2006). High-resolution thermal inertia derived from the Thermal emission imaging system (THEMIS): Thermal model and applications. *Journal of Geophysical Research*, *111*, 1–22. https://doi.org/10.1029/2006je002735

Frey, H., & Schultz, R. A. (1988). Large impact basins and the mega-impact origin for the crustal dichotomy on Mars. *Geophysical Research Letters*, *15*, 229–232. https://doi.org/10.1029/gl015i003p00229

Frey, H. V. (2006). Impact constraints on, and a chronology for, major events in early Mars history. *Journal of Geophysical Research*, *111*, 1–11. https://doi.org/10.1029/2005je002449

Greeley, R., Theilig, E., Guest, J. E., Carr, M. H., Masursky, H., & Cutts, J. A. (1977). Geology of Chryse Planitia. *Journal of Geophysical Research*, *82*, 4093–4109. https://doi.org/10.1029/js082i028p04093

Grotzinger, J. P., & Milliken, R. E. (2012). *The sedimentary rock record of Mars: Distribution, origins, and global stratigraphy*. SEPM Special Publications. https://doi.org/10.2110/pec.12.102.0001

Hauber, E., Gwinner, K., Kleinhans, M., Reiss, D., Di Achille, G., Ori, G.-G., et al. (2009). Sedimentary deposits in Xanthe Terra: Implications for the ancient climate on Mars. *Planetary and Space Science*, *57*, 944–957. https://doi.org/10.1016/j.pss.2008.06.009

Hynek, B. M., Arvidson, R. E., & Phillips, R. J. (2002). Geologic setting and origin of Terra Meridiani hematite deposit on Mars. *Journal of Geophysical Research*, *107*(10), 18–21. https://doi.org/10.1029/2002je001891

Jaumann, R., Neukum, G., Behnke, T., Duxbury, T. C., Eichentopf, K., Flohrer, J., et al. (2007). The high-resolution stereo camera (HRSC) experiment on Mars Express: Instrument aspects and experiment conduct from interplanetary cruise through the nominal mission. *Planetary and Space Science*, *55*, 928–952. https://doi.org/10.1016/j.pss.2006.12.003

Kersten, E., Gwinner, K., Michael, G., Bostelmann, J., Dumke, A., Wählisch, M., et al. (2018). *Topographic mapping of the Mars MC quadrangles using HRSC data* (Vol. 12, pp. 4–5). European Planetary Science Congress.

Kneissl, T., Van Gasselt, S., & Neukum, G. (2011). Map-projection-independent crater size-frequency determination in GIS environments: New software tool for ArcGIS. *Planetary and Space Science*, *59*, 1243–1254. https://doi.org/10.1016/j.pss.2010.03.015

Komatsu, G., Okubo, C. H., Wray, J. J., Ojha, L., Cardinale, M., Murana, A., et al. (2016). Small edifice features in Chryse Planitia, Mars: Assessment of a mud volcano hypothesis. *Icarus*, *268*, 56–75. https://doi.org/10.1016/j.icarus.2015.12.032

Loizeau, D., Mangold, N., Grant, J., Ansan, V., & Bibring, J. (2011). Stratigraphy of the clay-unit at Mawrth Vallis. *Mars*, *6*, 6–7.

Loizeau, D., Mangold, N., Poulet, F., Bibring, J. P., Gendrin, A., Ansan, V., et al. (2007). Phyllosilicates in the Mawrth Vallis region of Mars. *Journal of Geophysical Research*, *112*(8), 1–20. https://doi.org/10.1029/2006je002877

Loizeau, D., Werner, S. C., Mangold, N., Bibring, J.-P., & Vago, J. L. (2012). Chronology of deposition and alteration in the Mawrth Vallis region, Mars. *Planetary and Space Science*, *72*, 31–43. https://doi.org/10.1016/j.pss.2012.06.023

Malin, M. C., Bell, J. F., Cantor, B. A., Caplinger, M. A., Calvin, W. M., Clancy, R. T., et al. (2007). Context camera investigation on board the Mars reconnaissance orbiter. *Journal of Geophysical Research*, *112*, 1–25. https://doi.org/10.1029/2006je002808

Malin, M. C., & Edgett, K. S. (2000). Sedimentary rocks of early Mars. *Science*, *290*, 1927–1937. https://doi.org/10.1126/science.290.5498.1927

McEwen, A. S., Eliason, E. M., Bergstrom, J. W., Bridges, N. T., Hansen, C. J., Delamere, W. A., et al. (2007). Mars reconnaissance orbiter's high resolution imaging science experiment (HiRISE). *Journal of Geophysical Research*, *112*(5), 1–40. https://doi.org/10.1029/2005je002605. https://doi.org/10.1029/2005JE002605

McNeil, J., Fawdon, P., Balme, M., & Coe, A. L. (2021). *Chryse Planitia, Mars: Mound morphometry and morphology datasets*. The Open University. https://doi.org/10.21954/ou.rd.13675369.v1

Michalski, J. R., Bibring, J.-P., Poulet, F., Loizeau, D., Mangold, N., Dobrea, E. N., et al. (2010). The Mawrth Vallis region of Mars: A potential landing site for the Mars Science Laboratory (MSL) mission. *Astrobiology*, *10*, 687–703. https://doi.org/10.1089/ast.2010.0491

Michalski, J. R., Niles, P. B., Cuadros, J., & Baldridge, A. M. (2013). Multiple working hypotheses for the formation of compositional stratigraphy on mars: Insights from the Mawrth Vallis region. *Icarus*, *226*, 816–840. https://doi.org/10.1016/j.icarus.2013.05.024

Michalski, J. R., & Noe Dobrea, E. Z. (2007). Evidence for a sedimentary origin of clay minerals in the Mawrth Vallis region, Mars. *Geology*, *35*, 951–954. https://doi.org/10.1130/g23854a.1

Migoń, P. (2004). Mesa, Butte. In *Encyclopedia of geomorphology* (1st ed., pp. 106–107). London: Routledge.

Noe Dobrea, E. Z., Bishop, J. L., McKeown, N. K., Fu, R., Rossi, C. M., Michalski, J. R., et al. (2010). Mineralogy and stratigraphy of phyllosilicate-bearing and dark mantling units in the greater Mawrth Vallis/west Arabia Terra area: Constraints on geological origin. *Journal of Geophysical Research*, *115*. https://doi.org/10.1029/2009je003351

Noe Dobrea, E. Z., McKeown, N. K., Bishop, J. L., & Silver, E. (2009). Phyllosilicate diversity and past aqueous activity revealed at Mawrth Vallis, Mars. *40th lunar and planetary science conference* (pp. 830–833). https://doi.org/10.1126/science.1159699

Oehler, D. Z., & Allen, C. C. (2010). Evidence for pervasive mud volcanism in Acidalia Planitia, Mars. *Icarus*, *208*, 636–657. https://doi.org/10.1016/j.icarus.2010.03.031

Ormö, J., Komatsu, G., Chan, M. A., Beitler, B., & Parry, W. T. (2004).Geological features indicative of processes related to the hematite formation in Meridiani Planum and Aram Chaos, Mars: A comparison with diagenetic hematite deposits in southern Utah, USA. *Icarus*, *171*, 295–316. https://doi.org/10.1016/j.icarus.2004.06.001

Pan, L., Ehlmann, B. L., Carter, J., & Ernst, C. M. (2017). The stratigraphy and history of Mars' northern lowlands through mineralogy of impact craters: A comprehensive survey. *Journal of Geophysical Research: Planets*, *122*, 1824–1854. https://doi.org/10.1002/2017je005276

Pan, L., Quantin-Nataf, C., Breton, S., & Michaut, C. (2019). The impact origin and evolution of Chryse Planitia on Mars revealed by buried craters. *Nature Communications*, *10*, 1–8. https://doi.org/10.1038/s41467-019-12162-0

Phillips, R. J., Zuber, M. T., Solomon, S. C., Golombek, M. P., Jakosky, B. M., Banerdt, W. B., et al. (2001). Ancient geodynamics and global-scale hydrology on Mars. *Science*, *291*, 2587–2591. https://doi.org/10.1126/science.1058701

Poulet, F., Gross, C., Horgan, B., Loizeau, D., Bishop, J. L., Carter, J., & Orgel, C. (2020). Mawrth Vallis, Mars: A fascinating place for future in situ exploration. *Astrobiology*, *20*, 199–234. https://doi.org/10.1089/ast.2019.2074

Poulet, F., Mangold, N., Loizeau, D., Bibring, J., Langevin, Y., Michalski, J., & Gondet, B. (2008). Abundance of minerals in the phyllosilicate-rich units on Mars. *Astronomy & Astrophysics*, *44*, 41–45. https://doi.org/10.1051/0004-6361:200810150

Quantin-Nataf, C., Carter, J., Mandon, L., Thollot, P., Balme, M., Volat, M., et al. (2021). Oxia Planum: The landing site for the ExoMars "Rosalind Franklin" Rover Mission: Geological context and prelanding interpretation. *Astrobiology*, *21*. https://doi.org/10.1089/ast.2019.2191

Rodríguez, J. A. P., Tanaka, K. L., Kargel, J. S., Dohm, J. M., Kuzmin, R., Fairén, A. G., et al. (2007). Formation and disruption of aquifers in southwestern Chryse Planitia, Mars. *Icarus*, *191*, 545–567. https://doi.org/10.1016/j.icarus.2007.05.021

Rotto, S. L., & Tanaka, K. L. (1991). Geologic history and channeling episodes of the Chryse Planitia region of Mars (abstract). *Lunar planetary science conference XXII* (Vol. 22, pp. 1135–1136).

Rotto, S., & Tanaka, K. L. (1995). *Geologic/geomorphologic map of the Chryse Planitia region of Mars (1:5,000,000)*. USGS. https://doi.org/10.3133/i2441

Schultz, P. H., Schultz, R. A., & Rogers, J. (1982). The structure and evolution of ancient impact basins on Mars. *Journal of Geophysical Research*, *87*, 9803. https://doi.org/10.1029/jb087ib12p09803

Sefton-Nash, E., Balme, M., Quantin-Nataf, C., Fawdon, P., Volat, M., Hauber, E., et al. (2020). HiRISE scale characterization of the Oxia Planum landing site for the ExoMars Rosalind Franklin rover. *51st lunar and planetary science conference abstract*. https://doi.org/10.5194/epsc2020-978

Tanaka, K. L., Skinner, J. A., & Hare, T. M. (2005). *Geologic map of the northern plains of Mars*. U.S. Geological Survey. https://pubs.usgs.gov/sim/2005/2888/

Treiman, A. H. (2008). Ancient groundwater flow in the Valles Marineris on Mars inferred from fault trace ridges. *Nature Geoscience*, *1*, 181–183. https://doi.org/10.1038/ngeo131

Vago, J. L., Westall, F., Pasteur Instrument Teams, Coates, A. J., Jaumann, R., Korablev, O., et al. (2017). Habitability on early Mars and the search for biosignatures with the ExoMars rover. *Astrobiology*, *17*, 471–510. https://doi.org/10.1089/ast.2016.1533

Wagh, V., & Tarrer, A. R. (1991). *The effect of the physical and chemical characteristics of the aggregate on bonding* (1–23). Strategic Highway Research Program, National Research Council.

Werner, S. C. (2009). The global martian volcanic evolutionary history. *Icarus*, *201*(1), 44–68. https://doi.org/10.1016/j.icarus.2008.12.019

Yasir, S. F., Awang, H., & Ayub, M. I. H. (2018). The relationship of sandstone's strength with mineral content and petrographic characteristics in Sungai Tekai, Jerantut, Pahang. *AIP Conference Proceedings*, *2020*, 020010. https://doi.org/10.1063/1.5062636

Zuber, M. T., Smith, D. E., Solomon, S. C., Muhleman, D. O., Head, J. W., Garvin, J. B., et al. (1992). The Mars Observer laser altimeter investigation. *Journal of Geophysical Research*, *97*, 7781–7797. https://doi.org/10.1029/92je00341